

# Interpreting body MRI cases: what you need to know to get started

Flavius F. Guglielmo, Leann M. Kania, Hassan M. Ahmad, Christopher G. Roth, Donald G. Mitchell

Department of Radiology, Thomas Jefferson University, 132 South 10th Street, Philadelphia, PA 19107, USA

## Abstract

Interpreting body MRI cases can seem overwhelming to an uninitiated radiologist. The standard study includes a variety of pulse sequences, the names of which vary depending on the MR vendor. Pulse sequences may be displayed haphazardly on the picture archiving and communication system (PACS), frequently not synchronized with the imaging protocol. Adding to the complexity is the use of different gadolinium-based contrast agents, which may affect the timing and diagnostic yield of each sequence. The following introductory primer for interpreting body MRI cases is meant to create a basic framework for efficiently reviewing body MRI cases to provide high quality interpretations, fully utilizing the diagnostic information of the modality. There are 4 components that need to be mastered when interpreting body MRI cases including: (1) recognizing the key sequences in a basic body MRI protocol, (2) learning how to best display the key pulse sequences on PACS, (3) understanding the technique and clinical utility of each sequence and learning how to utilize sequences to be an “MR Pathologist”, and (4) understanding the key features of the different gadolinium based contrast agents.

**Key words:** Magnetic resonance imaging—MRI protocol—MRI case interpretation—Pulse sequences—MRI tissue characterization—Gadolinium

## Basic abdominal MRI protocol

Comprehensive evaluation for most abdominal applications is possible by performing a basic abdominal MRI protocol as illustrated in Fig. 1. In this protocol, the order of pulse sequences is optimized for extracellular space

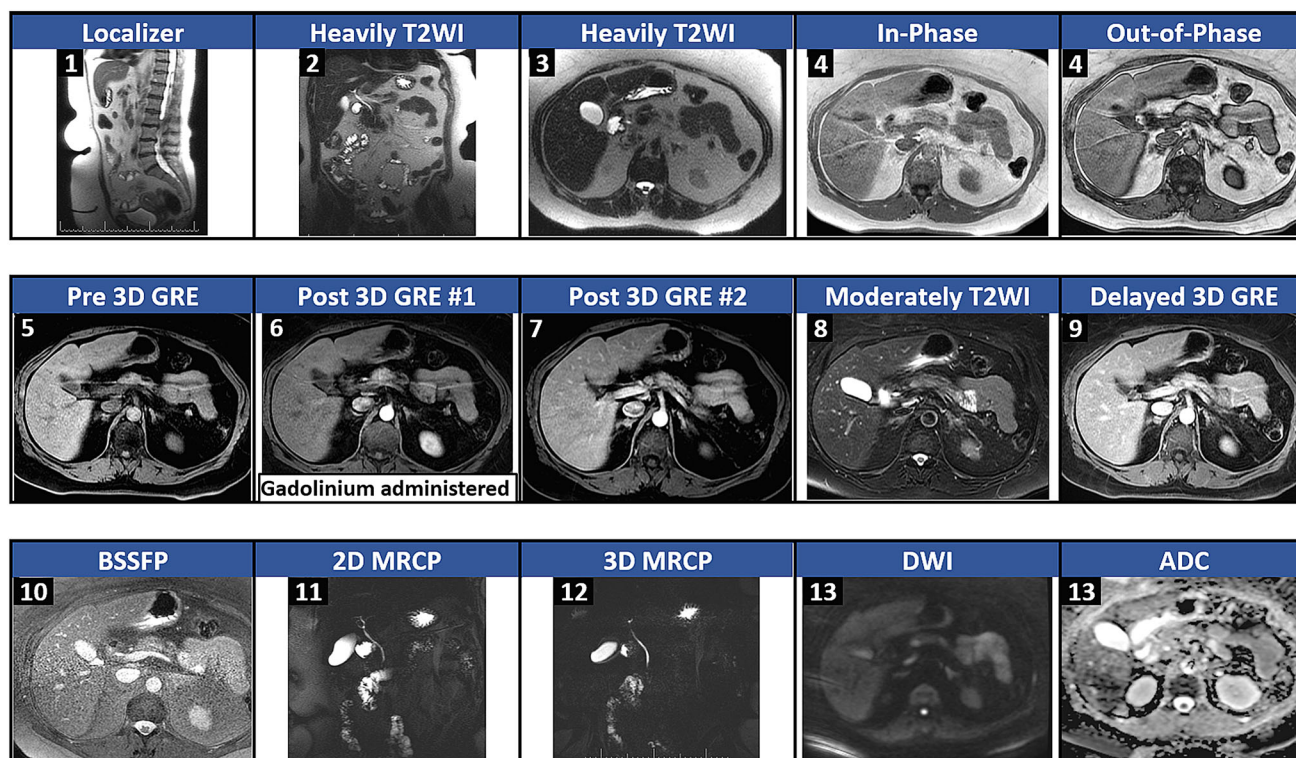
contrast agents. Protocol adjustments are needed when using the hepatocyte-specific contrast agent, gadoxetate disodium (Eovist/Primovist; Bayer HealthCare, Leverkusen, Germany) [1, 2]. The imaging parameters for the pulse sequences in this suggested protocol are listed in Table 1 along with the required protocol adjustments for gadoxetate disodium. Regarding contrast-enhanced protocols, an important point to remember is to administer gadolinium as early as possible, in case the patient cannot finish the exam. This ensures that the 3D pre- and post-gadolinium gradient echo sequences, often the most important pulse sequences, are performed (Fig. 1). This is feasible since (as discussed later) only heavily T2-weighted and dual gradient echo sequences need to be performed before gadolinium administration [2].

## How to recognize pulse sequences

While selected pulse sequences such as magnetic resonance cholangiopancreatography (MRCP) and diffusion-weighted images are universally recognizable, for an inexperienced radiologist, recognizing and discerning between T1-weighted, T2-weighted and balanced steady-state free precession (BSSFP) pulse sequences can be challenging. Non-standardized and proprietary vendor-specific naming of pulse sequences adds to the difficulty. While being familiar with the assortment of pulse sequence acronyms that exist is necessary, such as balanced fast-field echo (BFFE) or fast imaging employing steady-state acquisition (FIESTA), it is more important to be able to quickly recognize each pulse sequence. The following guidelines can be used to stratify pulse sequences into broad categories. To identify the pulse sequence, evaluate the signal intensity of fluid (e.g., CSF), and large blood vessels (e.g., abdominal aorta, inferior vena cava, and portal vein) in the image (Fig. 2).

- In T1-weighted images (T1WI), on noncontrast studies, both fluid and large blood vessels are dark.
- In T2-weighted images (T2WI), fluid is bright and large blood vessels are dark.

Correspondence to: Flavius F. Guglielmo; email: flavius.guglielmo@jefferson.edu



**Fig. 1.** This is a basic abdominal MRI protocol when using an extracellular space agent and the order of pulse sequence acquisition. This protocol can provide comprehensive evaluation for most abdominal applications. Specific parameters for this protocol are listed in Table 1. *2D* two dimensional, *3D* three dimensional, *ADC* apparent

diffusion coefficient, *BSSFP* balanced steady-state free precession, *DWI* diffusion-weighted imaging, *GRE* gradient echo, *MRCP* magnetic resonance cholangiopancreatography, *Post* dynamic postgadolinium, *Pre* pregadolinium, *T2WI* T2-weighted image.

- In balanced steady-state free precession (BSSFP) images, fluid and all blood vessels are bright (Fig. 2).

## PACS pulse sequence display

Due to the large variety of pulse sequences and the difficulty in creating standardized abdominal MRI hanging protocols on many picture archiving and communication systems (PACS), when an exam is first opened, pulse sequences may be displayed on PACS in an incompletely organized manner. When this occurs, a key component in accurate interpretation is appropriately reordering pulse sequences. The most important sequences to reorder are the pre- and postgadolinium fat-suppressed 3D gradient echo sequences which are usually crucial when making a diagnosis. Setting these up so that they can be viewed together and optimally compared should take no more than 1–2 min. Figure 3 shows an example of the original pulse sequence display on PACS and how pulse sequences were subsequently reordered on PACS to facilitate case interpretation in a patient with hepatocellular carcinoma.

## Abdominal MRI pulse sequences

When interpreting abdominal MRI exams, it is important to have a basic understanding of the technique and clinical utility of each pulse sequence. This information often enables the interpreting radiologist to make specific pathologic diagnoses as an “MR Pathologist” and readily identify many classic “Aunt Minnie” findings. The following discussion highlights each pulse sequence in a basic abdominal MRI protocol. The clinical utility of the pulse sequences discussed is summarized in Table 4 which appears at the end of this article (Table 4).

### Localizer series

#### Technique

Several different pulse sequences are used for this series including balanced steady-state free precession (BSSFP), single-shot fast spin echo (SSFSE), or T1-weighted images. This series is commonly obtained in 3 planes including sagittal, coronal, and axial. The default MR vendor series usually uses a large slice thickness (15 mm)

**Table 1.** A suggested basic abdominal MRI protocol when using an extracellular space agent (ECSA) and additional pulse sequences and parameters when using gadoxetate disodium instead of an ECSA

Sequence (in acquisition order)	Plane	FOV	Matrix	PAF	Slice thickness/ gap	TR (ms)	TE (ms)	Flip angle	Fat Suppression
Suggested basic abdominal MRI protocol when using an extracellular space agent (ECSA)									
SSFSE survey	3 plane	48	320 × 192	0	8/0	Min	80	90	No
Heavily T2WI	Coronal	44	256 × 192	1.7	5/0	Min	180	90	No
Heavily T2WI	Axial	38	256 × 192	2	5/0	Min	180	90	No
2D dual gradient echo in- and out-of-phase <sup>a</sup>	Axial	38	256 × 192	2	7/0.5	265	2.1/4.4	90	No
3D GRE (pre-contrast, late arterial, and portal venous phase)	Axial	42	320 × 224	1.8	4.4/2.2	Min	Min	12	Yes
Moderately T2WI FS	Axial	40	256 × 192	2	7.5/0.5	2300	84	90	Yes
3D GRE (delayed phase <sup>b</sup> )	Axial	42	320 × 224	1.8	4.4/2.2	Min	Min	15	Yes
BSSFP	Axial	38	192 × 288	2	5/0	Min	Min	70	Yes
2D MRCP <sup>c</sup>	Coronal	26	288 × 256	0	40/0	2666	1096	90	Yes
3D MRCP <sup>d</sup>	Coronal	38	320 × 320	2	1.4/0.7	3750	847	90	Yes
Diffusion-weighted imaging	Axial	36	128 × 128	2	6/1	7000	73	90	Yes
Additional postgadolinium pulse sequences and parameters when using gadoxetate disodium instead of an ECSA									
3D GRE (hepatobiliary phase) <sup>e</sup>	Axial	40	288 × 160	1.8	5/2.5	Min	Min	25–30	Yes
3D GRE (hepatobiliary phase) <sup>e</sup>	Coronal	42	288 × 160	0	5/2.5	Min	Min	25–30	Yes

2D two dimensional, 3D three dimensional, BSSFP balanced steady-state free precession, FOV field of view, FS fat suppressed, 3D GRE fat-suppressed 3D gradient echo, Min minimum, MRCP magnetic resonance cholangiopancreatography, ms milliseconds, PAF parallel imaging acquisition factor, SSFSE single-shot fast spin echo, T2WI T2-weighted image, TE echo time, TR repetition time

<sup>a</sup> The 2D Dual Gradient Echo In- and Out-of-phase series indicate a 2D acquisition. On modern MR equipment, a 2-point Dixon 3D acquisition is obtained which has parameters that match the “water” image used for the pre- and postgadolinium fat-suppressed 3D GRE series (except for the echo time)

<sup>b</sup> The “delayed phase” when using extracellular space contrast agents is called the “transitional phase” or “late dynamic phase” when using gadoxetate disodium

<sup>c</sup> 2D MRCP can be performed any time after administering an extracellular space contrast agent. With gadoxetate disodium, this series must be completed within 5 min after the injection to avoid image degradation from biliary excretion

<sup>d</sup> Due to biliary excretion and the long series acquisition time, 3D MRCP should be performed before gadoxetate disodium administration or not at all

<sup>e</sup> This series is generally performed 20 min after gadoxetate disodium injection

and large interslice gaps (10 mm), which limits the clinical utility of this series. However, this can be changed to thinner slices with minimal or no gaps to make this an effective initial survey series which can have diagnostic value.

### Clinical utility

This series helps the MR technologist to confirm torso array coil positioning over the liver or other organ of interest. With case interpretation, this may be the only series in which the spine is visualized in the sagittal plane which may be the best plane for identifying compression fractures or localizing spinal lesions (Fig. 4).

### Heavily T2-weighted images

#### Technique

“Heavily T2-weighted” is defined as an echo time (TE) of 180–200 ms [3]. The longer echo time compared with the “moderately T2-weighted” sequence (TE = 80–100 ms) makes this sequence more fluid sensitive and also improves tissue characterization when interpreted in conjunction with moderately T2-weighted images (discussed

below). This sequence is not fat suppressed, so that organ boundaries can be better delineated. Each slice is obtained in about 1 s making this series resistant to most motion artifacts [4]. The numerous and frequent 180° refocusing pulses also make this series more resistant to susceptibility artifact than any other series. Since the T2-shortening effects of gadolinium will darken the renal collecting systems and hepatic hemangiomas, this series should be performed before gadolinium administration [2, 5].

### Clinical utility

Structures containing simple fluid will have high signal intensity on this series including cysts, fluid collections, and edema. Within cysts, septations and mural nodules are readily identifiable. Solid tissues and areas of fibrosis will generally have low signal intensity (Fig. 5).

This series can be used as a quick screen for benign liver lesions. Cysts generally have high signal intensity approaching cerebrospinal fluid (CSF) while hemangiomas have signal intensity between that of CSF and spleen. Solid lesions, on the other hand, have signal intensity similar to spleen or may be inconspicuous on this series (Fig. 6) [3].



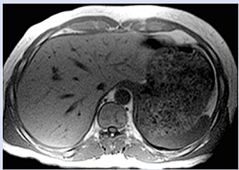



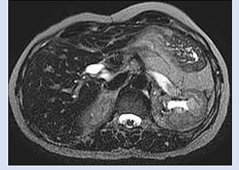

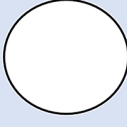



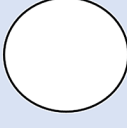
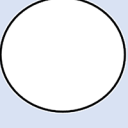
	Not Fat-Suppressed	Fat-Suppressed	Fluid	Blood Vessels
T1WI	 In-Phase dual GRE	 3D GRE		
T2WI	 Heavily T2W	 Moderately T2W FS		
BSSFP	 BFFE	 FIESTA		

Fig. 2. Diagram illustrating how to differentiate T1-weighted, T2-weighted, and balanced steady-state free precession pulse sequences. *3D GRE* fat-suppressed 3D gradient echo, *BFFE* balanced fast-field echo, *BSSFP* balanced steady-state

free precession, *FIESTA* fast imaging employing steady-state acquisition, *FS* fat suppressed, *T1W* T1 weighted, *T2W* T2 weighted.

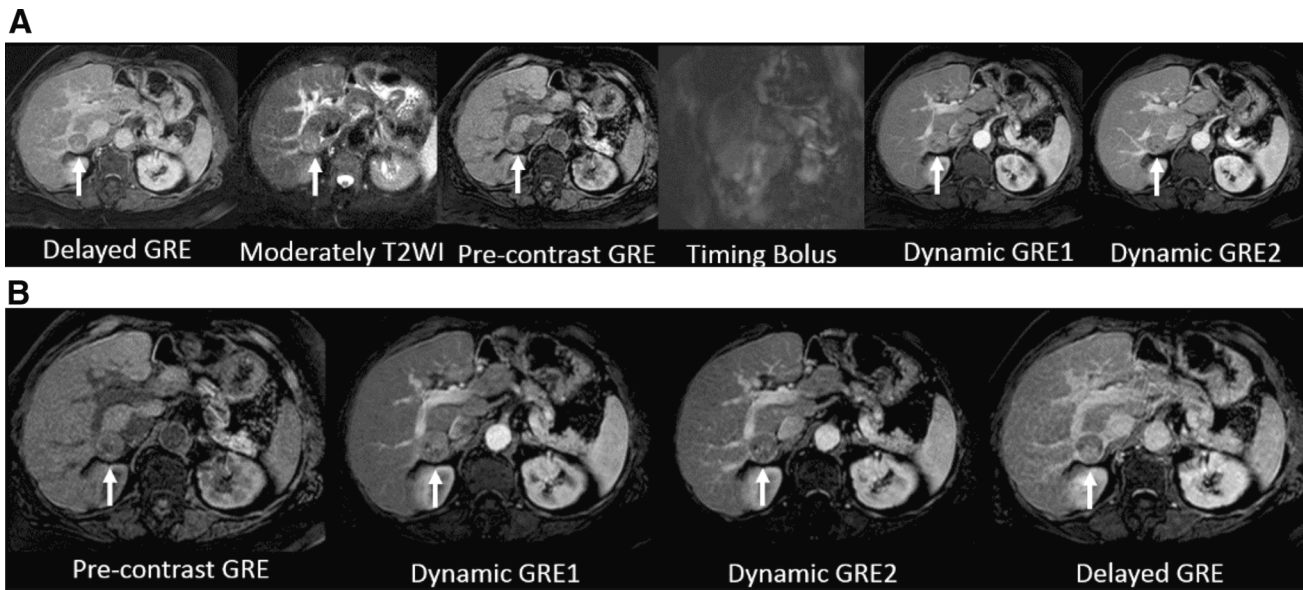
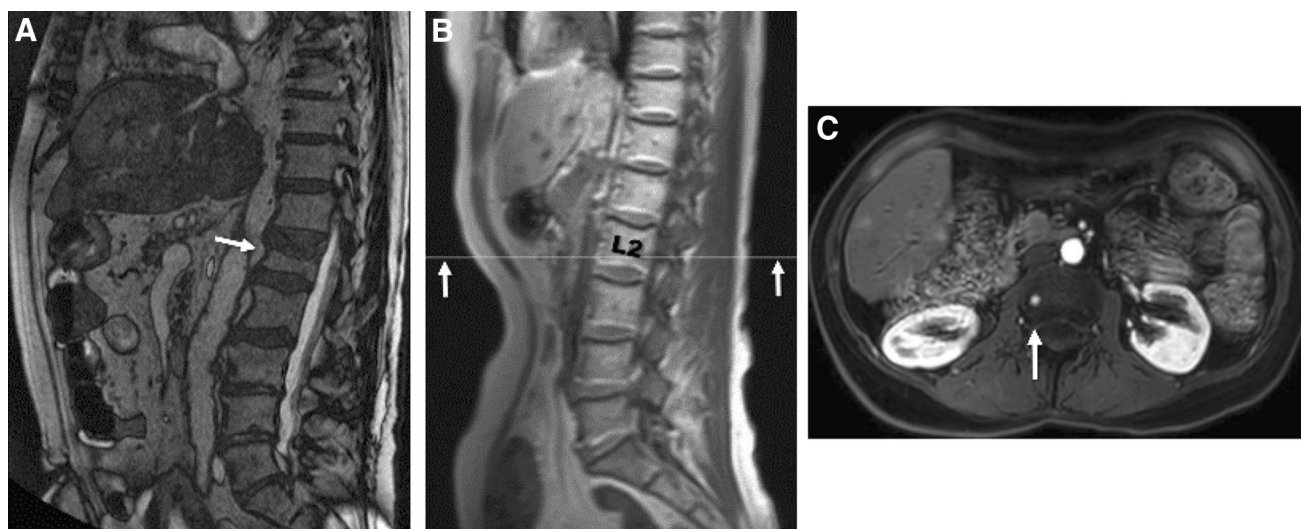


Fig. 3. **A** This is the original order of pulse sequences displayed on PACS in a patient with hepatocellular carcinoma (HCC). The delayed 3D gradient echo series was displayed before the precontrast and dynamic postcontrast 3D GRE series. **B** This was the order of pulse sequences after spending

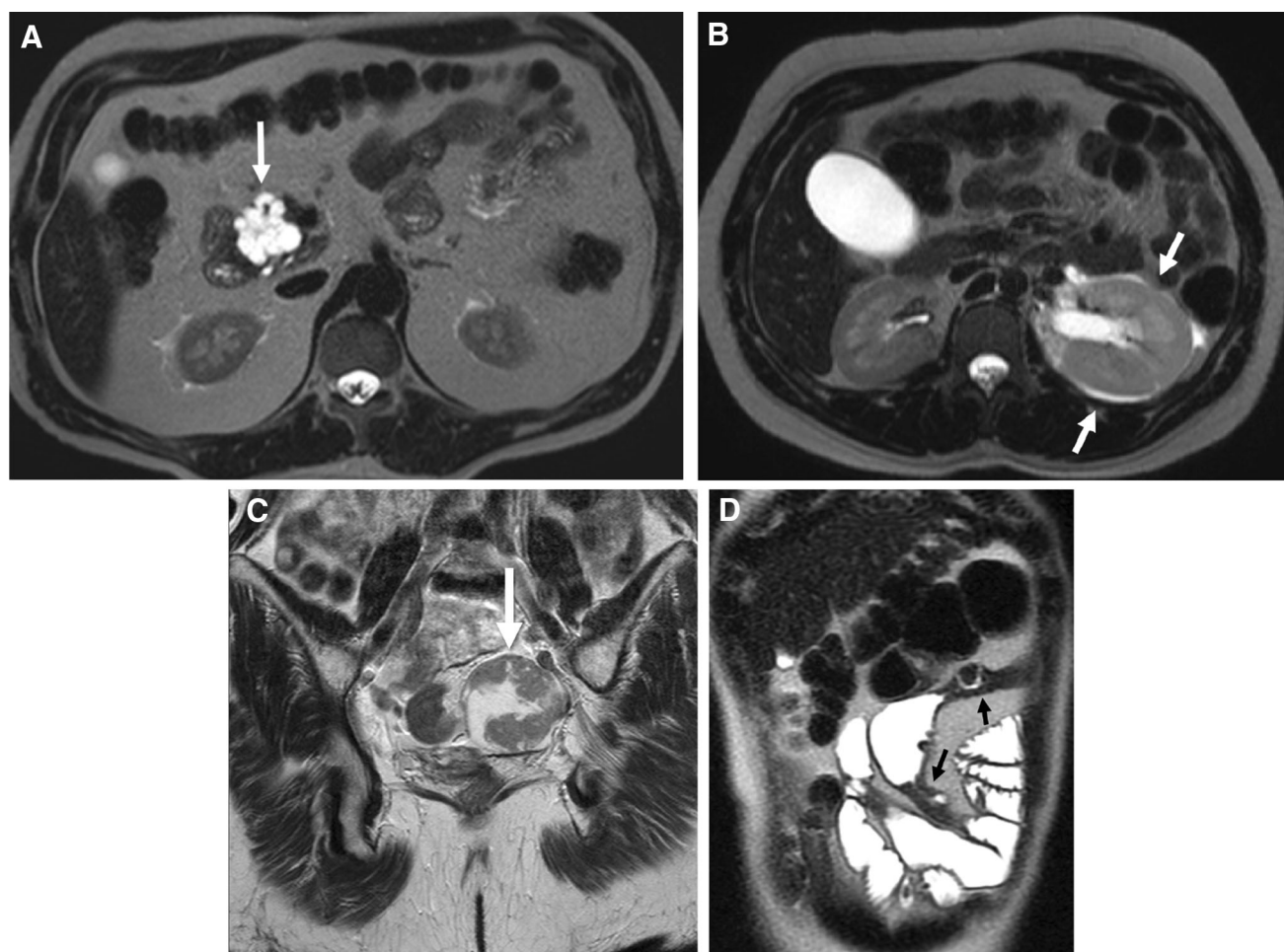
<1 min reordering the pulse sequences on PACS. The heterogeneous enhancement with washout and a capsule appearance in this HCC (*arrows*) is now more readily identified. *GRE* fat-suppressed 3D gradient echo, *PACS* picture archiving and communication system, *T2WI* T2-weighted image.





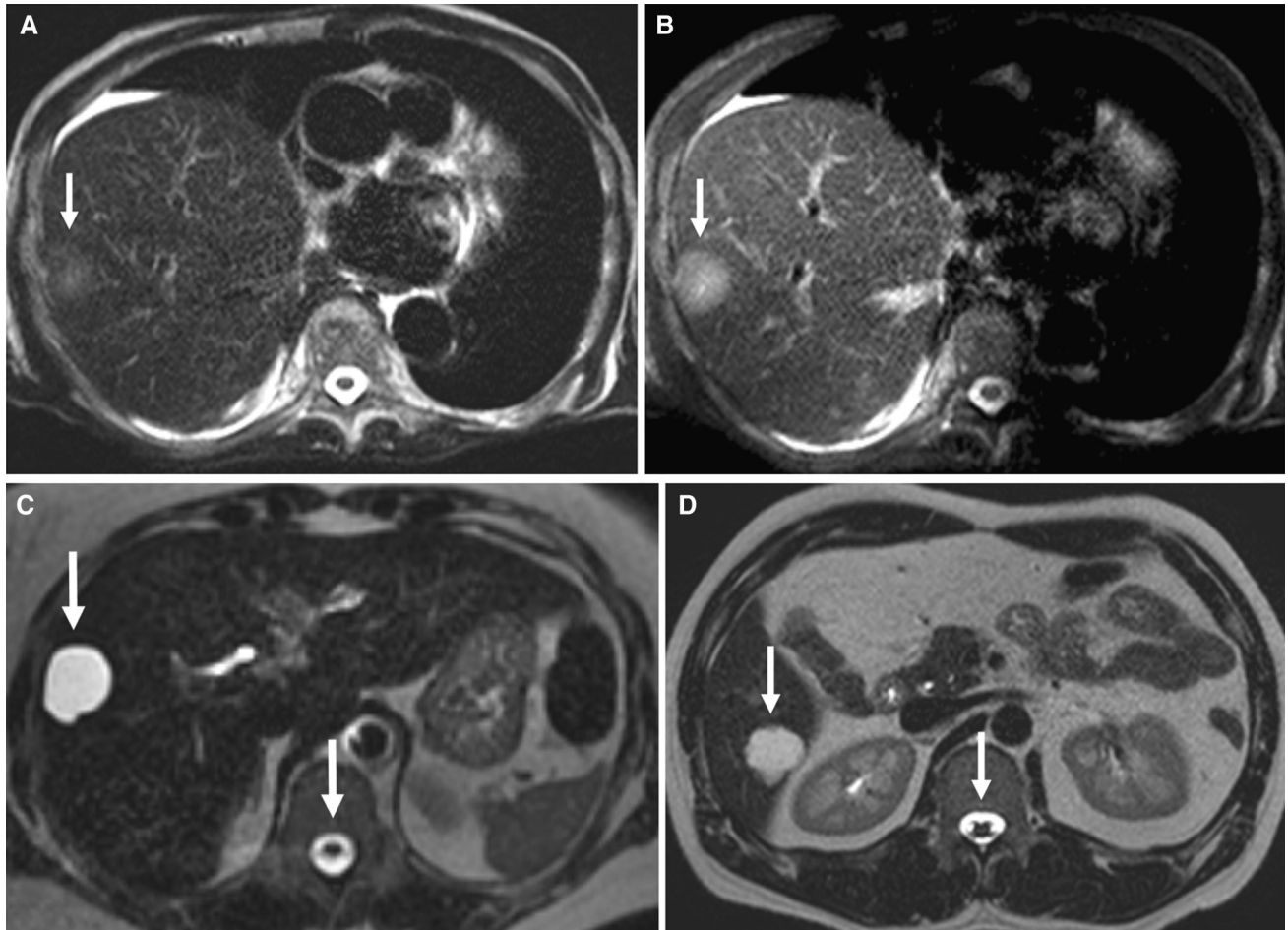
**Fig. 4.** **A** Balanced steady-state free precession localizer sequence showing a vertebral body compression fracture at L1 (*arrow*). **B** Sagittal T1-weighted localizer sequence and **C** axial 3D fat-suppressed gradient echo sequence which shows

a metastasis in the L2 vertebral body (*arrow* in **C**). Numbering of the vertebral segment on the axial image is facilitated by correlating with the sagittal localizer sequence.



**Fig. 5.** Heavily T2-weighted images (echo time 180 ms) showing the clinical utility of this pulse sequence in evaluating a pancreatic serous cystadenoma (*arrow* in **A**), left

pyelonephritis (*arrows* in **B**), mixed solid and cystic left ovarian neoplasm (*arrow* in **C**), and fibrotic small bowel strictures (*arrows* in **D**).

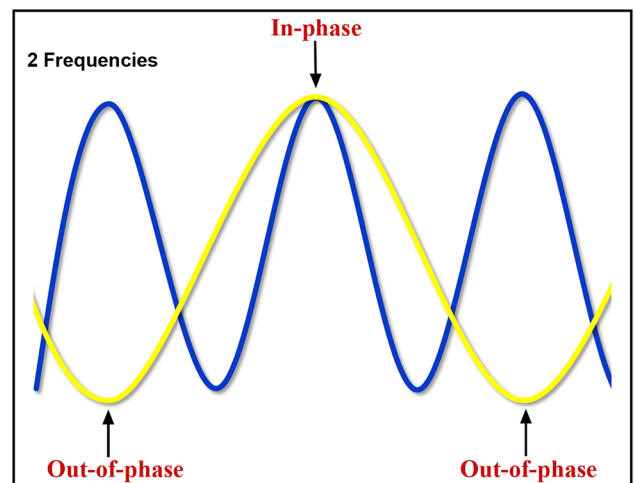


**Fig. 6.** **A** Heavily T2-weighted image (echo time 180 ms) showing a pancreatic adenocarcinoma metastasis which is nearly isointense to liver on the heavily T2-weighted image although is readily identified on the moderately T2-weighted image (echo time 80 ms) in **(B)**. **C** and **D** are heavily T2-

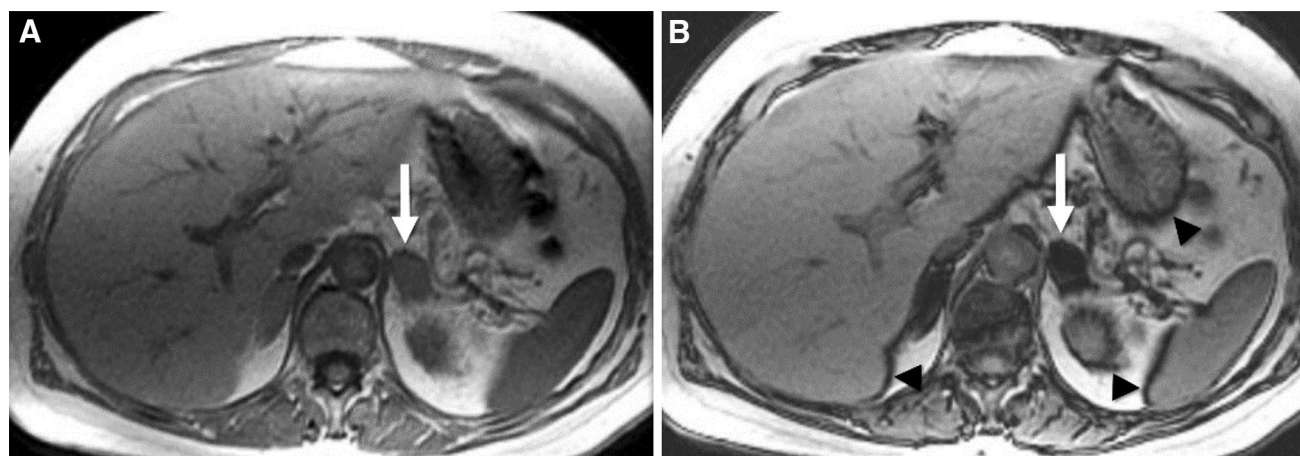
weighted images (echo time 180 ms). **C** shows high signal intensity in a hepatic cyst, similar to cerebrospinal fluid (CSF) signal intensity (arrows). **D** shows high signal intensity in a hepatic hemangioma, just lower than CSF signal intensity (arrows).



**Fig. 7.** Moderately T2-weighted image with an echo time of 80 ms showing a metastatic liver lesion from a gallbladder carcinoma (arrow). Note that the signal intensity of the metastatic lesion is similar to normal splenic signal intensity.













**Fig. 8.** The different frequencies of water (blue line) and fat (yellow line) are shown. When in-phase signal is summed, it results in high signal intensity. When out-of-phase signal is summed, signal cancellation results in low signal intensity.



**Fig. 9.** Images from an in-phase (**A**) and out-of-phase (**B**) dual gradient echo pulse sequence showing signal dropout on the out-of-phase image (relative to the in-phase image) due to

phase cancellation in a left adrenal adenoma (*arrows*). Also shown in (**B**) is a dark rim (*arrowheads*) at fat/water interfaces (“India ink artifact”) which is also due to phase cancellation.

Water	100%	75%	50%	25%	0%
Fat	0%	25%	50%	75%	100%
In-phase signal intensity					
Out-of-phase signal intensity					

**Fig. 10.** Diagram showing the change in signal intensity with various amounts of water and fat relative to each other. Maximal phase cancellation occurs when water and fat are

each 50%. Note that a 25%/75% fat/water mixture has the same signal intensity as a 75%/25% mixture and thus is ambiguous.

## Moderately T2-weighted images

### Technique

“Moderately T2-weighted” is defined as an echo time (TE) of 80–100 ms [3]. This series is ideally obtained with fat suppression to improve the dynamic range. This series should also be performed postgadolinium for the following reasons: (1) this allows the gadolinium contrast agent to be injected earlier in the protocol, (2) obtaining this series after dynamic imaging but before the delayed postcontrast 3D gradient echo series can help assure that this latter series is indeed “delayed”, and (3) the T1-shortening effects of gadolinium slightly increases the conspicuity of solid liver lesions and lymph nodes [6, 7].

### Clinical utility

This series is useful for identifying solid masses and lymph nodes [3]. As a general rule, similar to most pulse sequences, the signal intensity of liver metastasis and lymph nodes is similar to the signal intensity of a normal spleen (Fig. 7). This series is also useful for evaluating conditions with increased free water, such as inflammation (e.g., pancreatitis, pyelonephritis, etc.).

Evaluating lesions using both the moderately and heavily T2-weighted sequences helps with lesion characterization. Benign nonsolid lesions are generally bright relative to liver on both of the sequences. Malignant lesions are relatively bright compared to liver on moderately T2-weighted images, but nearly isointense to liver on heavily T2-weighted images (Fig. 6) [3, 5].



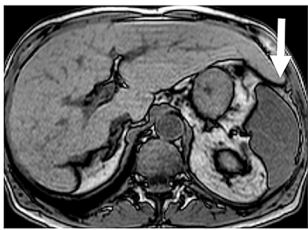

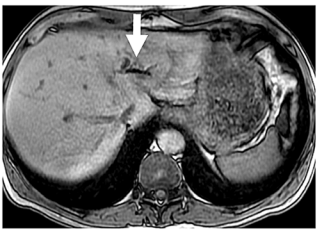

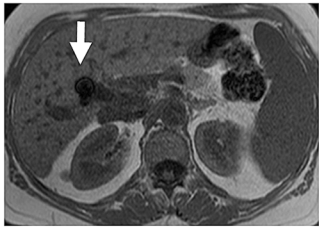
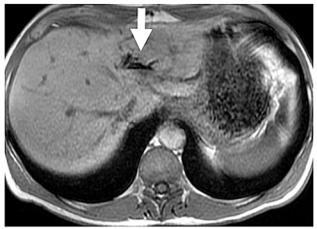
	Splenic Iron Overload	Cholecystectomy clips	Pneumobilia
<b>Out-of-phase (TE 2.3 msec)</b>			
<b>In-phase (TE 4.6 msec)</b>			

Fig. 11. Diagram showing the decrease in signal intensity between the out-of-phase and in-phase sequences related to the longer echo time of the in-phase sequence due to magnetic susceptibility effect from iron overload in the

spleen (left images, arrows), cholecystectomy surgical clips in the gallbladder fossa (middle images, arrows) and pneumobilia in the left hepatic lobe (right images, arrows) (TE echo time).

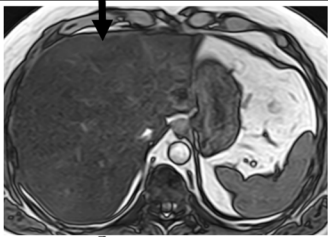
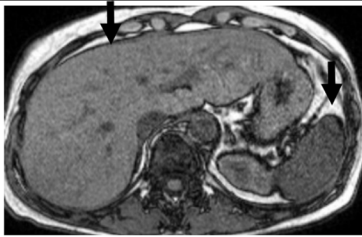
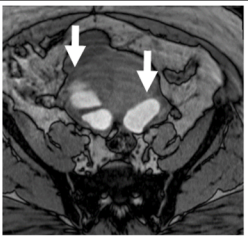
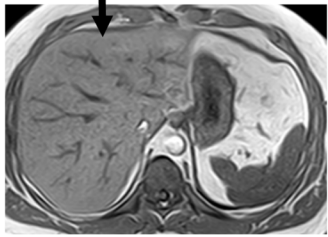
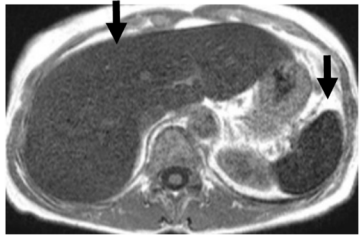
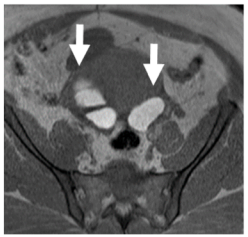
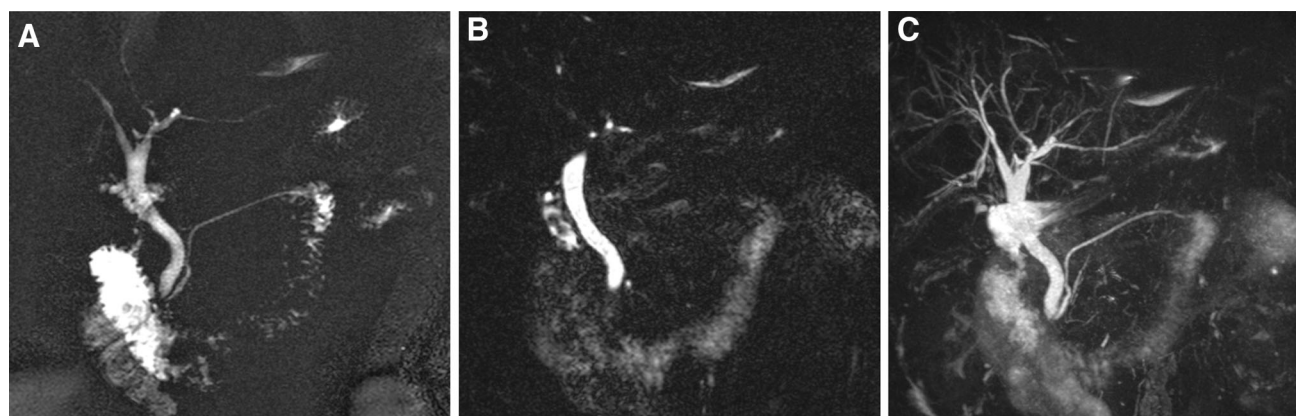
	Hepatic Steatosis	Hemosiderosis	Endometriosis
<b>Out-of-phase (TE 2.3 msec)</b>			
<b>In-phase (TE 4.6 msec)</b>			
	Identifies <u>water and fat in the same voxel</u> by decreased signal intensity on out-of-phase images	<u>Magnetic susceptibility effect</u> leads to decreased signal intensity on in-phase images	Substances with <u>short T1 values</u> such as blood or protein result in high signal intensity on both in-phase and out-of-phase images

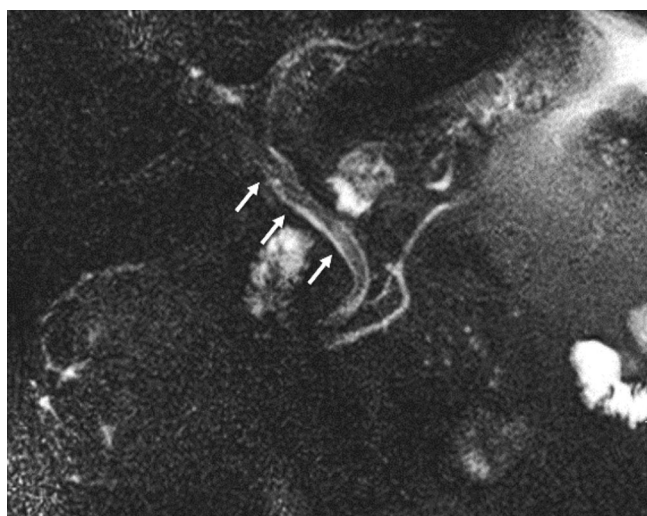
Fig. 12. Diagram showing how the difference in signal intensity, or lack of change in signal intensity, between the out-of-phase and in-phase sequence can be used to make specific pathologic diagnoses. In the left images, decreased out-of-phase signal intensity in the liver (relative to in-phase images) indicates hepatic steatosis (arrows); in the middle images, decreased in-phase

signal intensity in both the liver and spleen (relative to out-of-phase images) indicates iron deposition in both organs (arrows); and in the right images, high signal intensity in both adnexa on both the out-of-phase and in-phase images [without a drop in signal intensity on fat-suppressed images (not shown)] is diagnostic of bilateral endometriomas (arrows) (TE echo time).



**Fig. 13.** **A** is a single image from a rotating series of oblique longitudinal 40-mm slab 2D magnetic resonance cholangiopancreatography (MRCP) images. **B** is a single 1.6-mm

image from a 3D MRCP acquisition. The entire dataset is used to generate 3D MRCP MIP images such as **(C)**, which can be displayed as a rotating series.



**Fig. 14.** 2D magnetic resonance cholangiopancreatography image obtained 19 min after administering gadoxetate disodium. There is decreased signal intensity in the biliary system (arrows) due to biliary excretion of gadolinium related to the T2-shortening effects of gadolinium. This limits evaluation for biliary filling defects.

## Dual gradient echo in- and out-of-phase

### Technique

In this gradient echo pulse sequence, two different echo times are obtained that optimize the precessional frequency difference of water and fat. At specific echo times related to the magnetic field strength, fat and water signal is either in-phase or out-of-phase. When **in-phase** water and fat signal is summed, it results in high signal intensity. When **out-of-phase** water and fat signal is summed, signal cancellation results in low signal intensity (Fig. 8) [8–10].

Phase cancellation leads to decreased signal intensity on out-of-phase images (relative to in-phase images)

when tissues contain both fat and water, such as in adrenal adenomas or hepatic steatosis, and also leads to a dark band at fat/water interfaces, also known as “India ink” artifact (Fig. 9) [8–10].

In organs, the amount of fat relative to water determines how much decreased signal intensity will be present on out-of-phase images. Signal cancellation is maximal when water and fat are each 50% (Fig. 10) [5, 8–11].

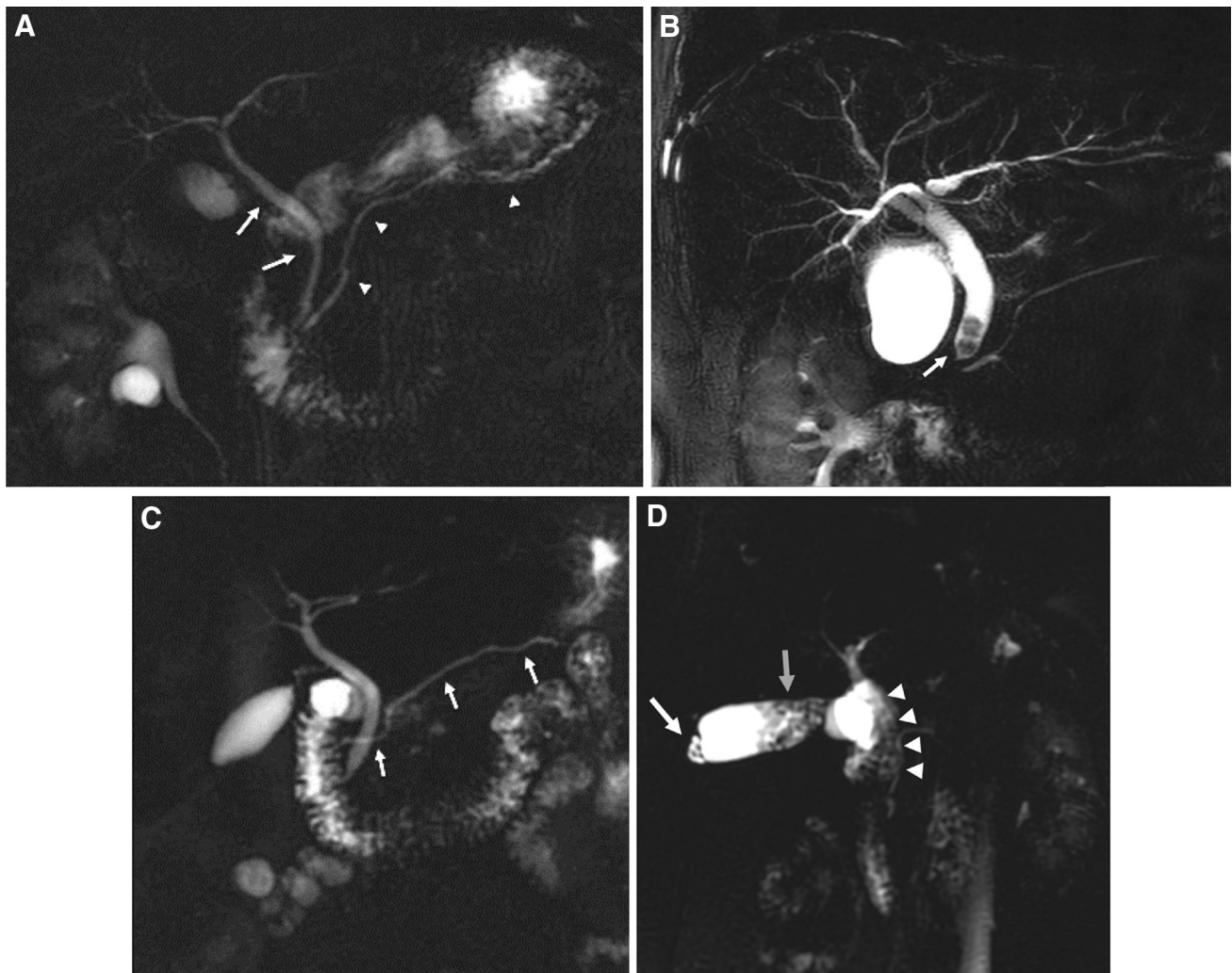
This series should be performed before gadolinium administration. Otherwise signal intensity differences between in-phase and out-of-phase images will be less conspicuous [2, 5].

### Clinical utility

This sequence is a simple yet powerful tool for tissue characterization. In addition to its value for showing fat content, the longer echo time of in-phase images compared to out-of-phase images causes decreased signal intensity in substances such as iron, calcium, metal objects, and air due to the magnetic susceptibility effect (Fig. 11) [12].

In many instances, specific pathologic diagnoses can be made by evaluating for a change or lack of change in signal intensity between the in- and out-of-phase series. For example, lower signal intensity on out-of-phase images (compared to in-phase images) is specific for mixed water and fat content and can diagnose hepatic steatosis or adrenal adenomas. Lower signal intensity on in-phase images (compared to out-of-phase images) can diagnose iron deposition in the spleen and liver. Finally, unchanged high signal intensity on both in-phase and out-of-phase images occurs with entirely fatty tissue or substances with short T1 values such as blood or protein, and can be used to diagnose conditions such as lipomas or endometriosis (Fig. 12) [8–13].





**Fig. 15.** 2D magnetic resonance cholangiopancreatography images. **A** shows a normal bile duct (arrows) and normal pancreatic duct (arrowhead). **B** shows two calculi in the distal common bile duct (arrow). **C** shows a pancreatic divisum

(arrows). **D** shows adenomyomatosis in the gallbladder fundus (white arrow) and common bile duct and common hepatic duct choledocholithiasis (arrowheads).

## 2D and high resolution 3D MRCP

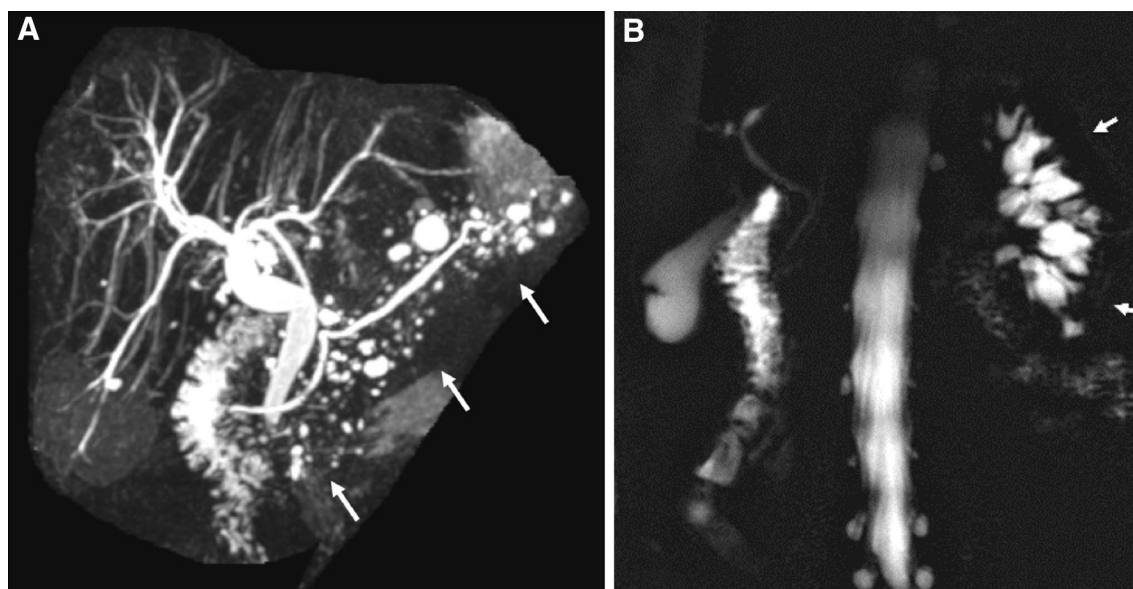
### Technique

MRCP sequences are extremely T2 weighted with an echo time (TE) of up to 800 ms or more. Both 2D and 3D MRCP can be performed. With 2D MRCP multiple sequential overlapping oblique 40–50 mm breath hold slabs are obtained. There should be a pause of 10 s between slices, to prevent saturation of fluid signal by the overlapping excitation pulses of the different slices. With 3D MRCP, a respiratory triggered volume is acquired, allowing reconstruction of overlapping slices at increments of about 1.5 mm, during a 3- to 5-min sequence. Rotating maximum intensity projection (MIP) images can then be created (Fig. 13) [14].

MRCP series are usually fat suppressed. Although gadolinium contrast is not needed for MRCP, if gadolinium is used, MRCP should ideally be performed after its administration. One reason for this is that the gadolinium T2-shortening effect decreases the signal intensity of the renal collecting systems and kidneys, and decreases background noise from vessels, which improves visualization of the bile ducts and pancreatic ducts [2, 5, 15]. Also, as discussed previously, any series that can be obtained after contrast administration should be, so that the gadolinium contrast can be administered as early as possible in the MRI protocol.

Protocol adjustments are needed when using the hepatocyte-specific contrast agent, gadoxetate disodium, which appears in the bile ducts as a function of its





**Fig. 16.** **A** Maximum intensity projection image from a 3D magnetic resonance cholangiopancreatography (MRCP) showing multiple side branch intraductal papillary mucinous neoplasms (arrows) and a pancreatic divisum. **B** 2D MRCP in

a patient with multiple left peripelvic renal cysts (arrows) readily identifiable on postgadolinium images due to the darkening of the kidney and collecting system by the gadolinium.

excretion which is nearly equally split between the renal and hepatobiliary systems. Consequently, MRCP pulse sequences must be timed to avoid the T2-shortening effects which eliminate signal from contrast-concentrating bile. Specifically, 2D MRCP must be performed within 5 min after injecting. 3D MRCP, due to its longer series acquisition time, should be performed precontrast or not at all to avoid darkening the bile ducts by biliary excretion (Fig. 14) [16].

#### *Clinical utility*

MRCP's main role is evaluation of the biliary system, the pancreatic duct, and the gallbladder (Fig. 15).

In addition, MRCP can be used to evaluate any fluid-filled or cystic structure in the abdomen (Fig 16).

#### *Diffusion-weighted imaging*

Diffusion-weighted imaging (DWI) is uniquely sensitive to water mobility within tissues. Tissues with decreased water diffusion, such as those with dense cellularity or tense edema, will show high signal on this pulse sequence relative to other tissues that show low signal due to water motion [17].

#### *Technique*

DWI is based on a single-shot echo planar technique, which is T2 weighted. These echo planar images are obtained with two or more  $b$  values. The higher the  $b$  value, the stronger the diffusion weighting. At many centers,  $b$  values of 0, 20, and 800 are routinely obtained.

$b$  values of 0 and 20 both provide T2-weighted information. A  $b$  value of 0 has no diffusion weighting. A  $b$  value of 20 provides minimal diffusion weighting, but sufficient so that bulk motion in blood vessels causes dramatic signal loss, so tumors, edema, and fluid are more conspicuous. A  $b$  value of 800 allows loss of signal from mobile water, increasing the conspicuity of tissues with restricted diffusion. When at least 2  $b$  values are obtained, an ADC map can be generated, depicting tissues with abundant diffusion as high signal which helps to identify "T2 shine-through" as opposed to true restricted diffusion, which has low signal on an ADC map (Figs. 17, 18).

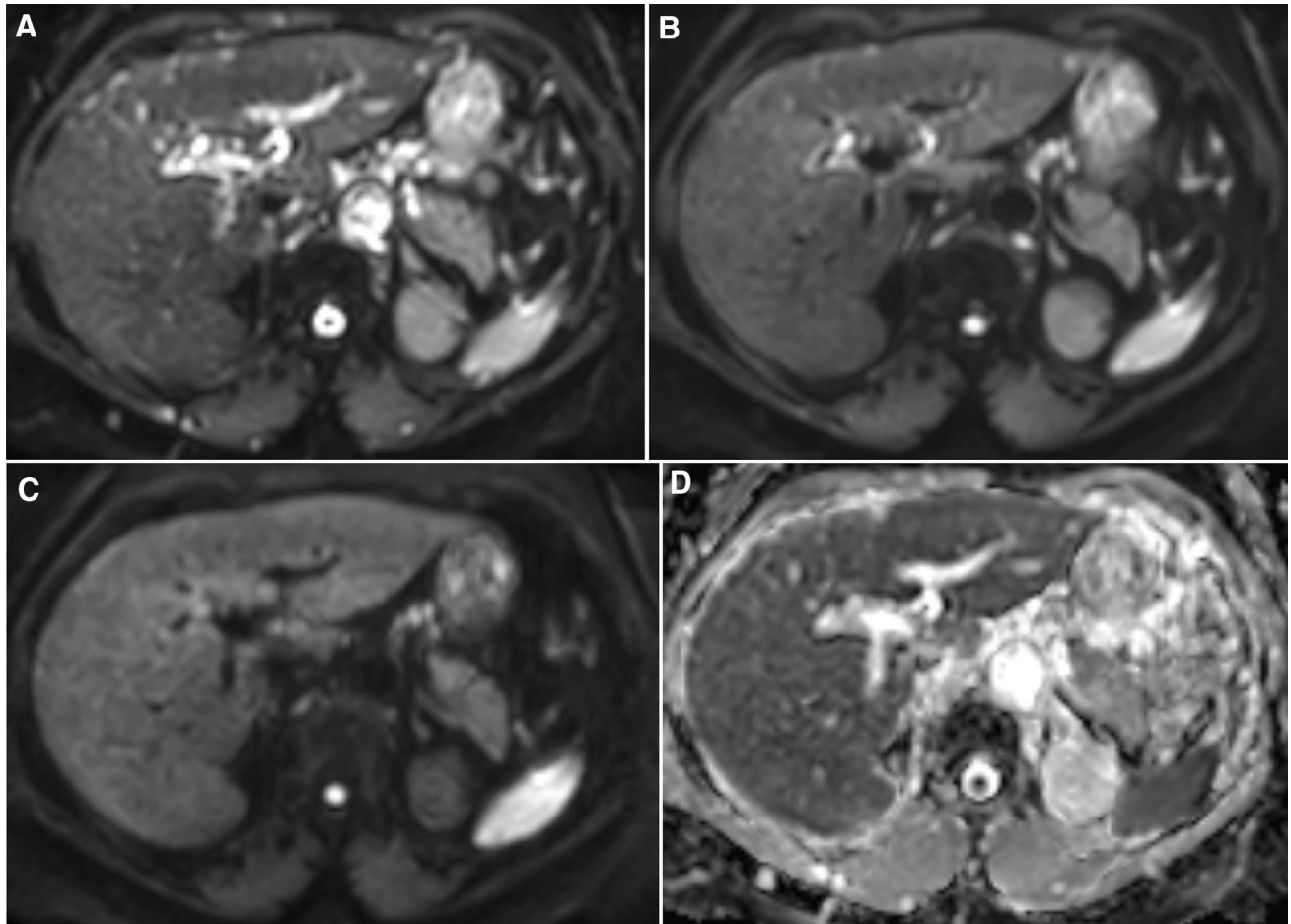
DWI sequences can be performed with breath holding, respiratory triggering, or free breathing with multiple averages (e.g., 4–10). The latter two approaches each generally take 3–6 min to complete, but free breathing has the highest signal to noise ratio (SNR) and reproducible suppression of respiratory motion. Breath hold techniques have variable success and are limited by SNR [18–21].

#### *Clinical utility*

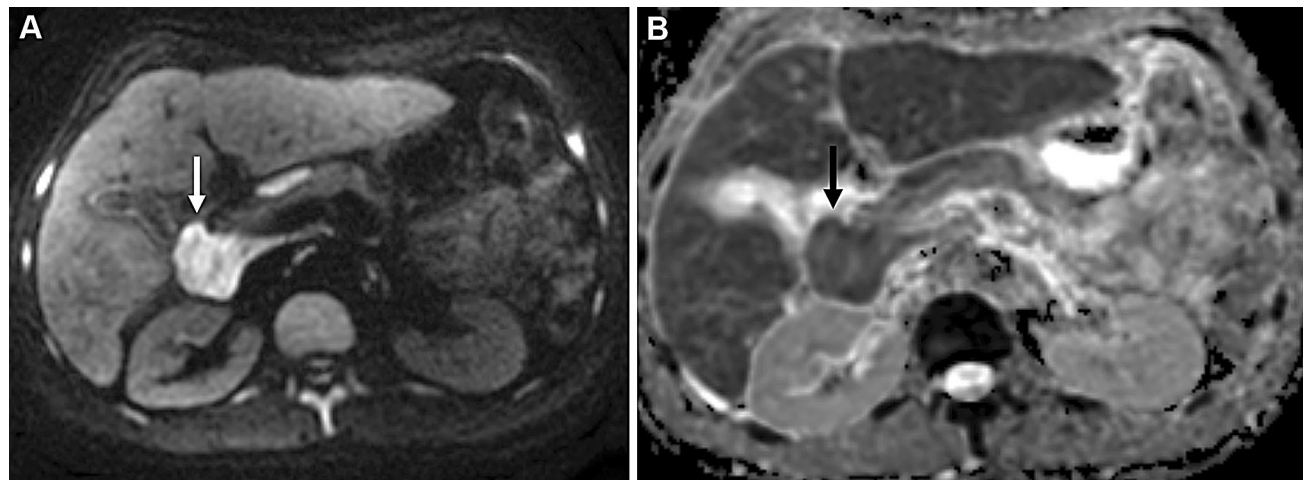
DWI is usually the best series for identifying lymph nodes (Fig. 18).

DWI may identify solid hepatic (and extrahepatic) malignancies that are not definable on other series (Fig. 19) [22].

Bone metastasis may be more conspicuous on DWI than other pulse sequences. The solid components of cystic lesions can be identified with DWI (Fig. 20).

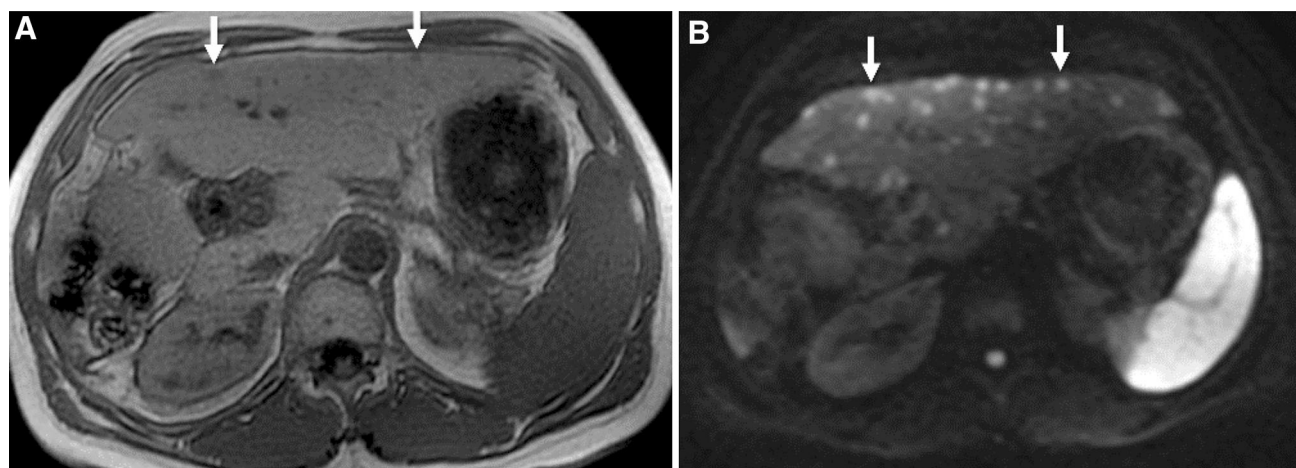


**Fig. 17.** Diffusion-weighted images showing  $b$  values of 0 (**A**), 20 (**B**), and 800 (**C**), obtained with multiple signal averages during free breathing, and the ADC Map (**D**) which is generated by the multiple  $b$  values.



**Fig. 18.** Diffusion-weighted image with a  $b$  value of 800 (**A**) and the corresponding ADC Map (**B**) showing an enlarged lymph node in the portacaval space in a patient with primary

sclerosing cholangitis (*arrows*) which has high signal intensity on the  $b$  800 image and low signal on the ADC map indicating restricted diffusion.



**Fig. 19.** Dual gradient echo in-phase image (A) and diffusion-weighted image (DWI) with a  $b$  value of 800 (B) in a patient with multifocal hepatocellular carcinoma. Multiple liver

lesions are nearly invisible on the in-phase image yet readily identifiable as hyperintense lesions on the DWI image (arrows).



**Fig. 20.** Diffusion-weighted sequence with  $b$  values of 0 (A) and 800 (B) and the corresponding ADC Map (C) showing restricted diffusion in the solid components of a right ovarian

mass in a patient with ovarian serous cystadenocarcinoma (arrows). The  $b$  value of 0 provides no diffusion weighting, while the  $b = 800$  image is diffusion weighted.

DWI sequences are especially important when gadolinium is not used, although diffusion restriction is not a complete substitute for the enhancement kinetics of solid tissue. A useful rule that applies to most pulse sequences, including DWI, is that most lymph nodes and solid lesions have signal intensity similar to that of a normal spleen.

DWI can also be used to identify normal structures. For example, normal adrenal glands and ovaries may be more conspicuous on DWI than other pulse sequences (Fig. 21).

### Balanced steady-state free precession

#### Technique

Balanced steady-state free precession (BSSFP) is a bright-blood technique in which all 3 gradients (i.e., frequency, phase, and slice) are refocused with each repetition time, and no spoiler gradients are applied [4, 23, 24]. This sequence is also known as balanced fast-field echo (BFFE), fast imaging employing steady-state

acquisition (FIESTA), and true fast imaging with steady-state precession (true FISP), depending on the MR vendor. This series can be performed with or without fat suppression (Fig. 22).

#### Clinical utility

BSSFP can be used as a 3 plane localizer or a separate diagnostic axial, sagittal, or coronal series. The short acquisition time of BSSFP and the complete balancing of all 3 imaging gradients make this the most motion resistant sequence. Due to its acquisition speed and lack of saturation effects from rapidly repeated excitations, BSSFP can be used to create the cine series for MR enterography exams, cardiac MRI exams, or any other exam to depict motion of blood or tissue [25].

Due to the insensitivity of this sequence to signal loss from motion, pericardial effusions are usually more conspicuous with BSSFP than T2-weighted images (T2WI), due to the flow void artifact created on T2WI by adjacent cardiac wall motion (Fig. 23) [26].



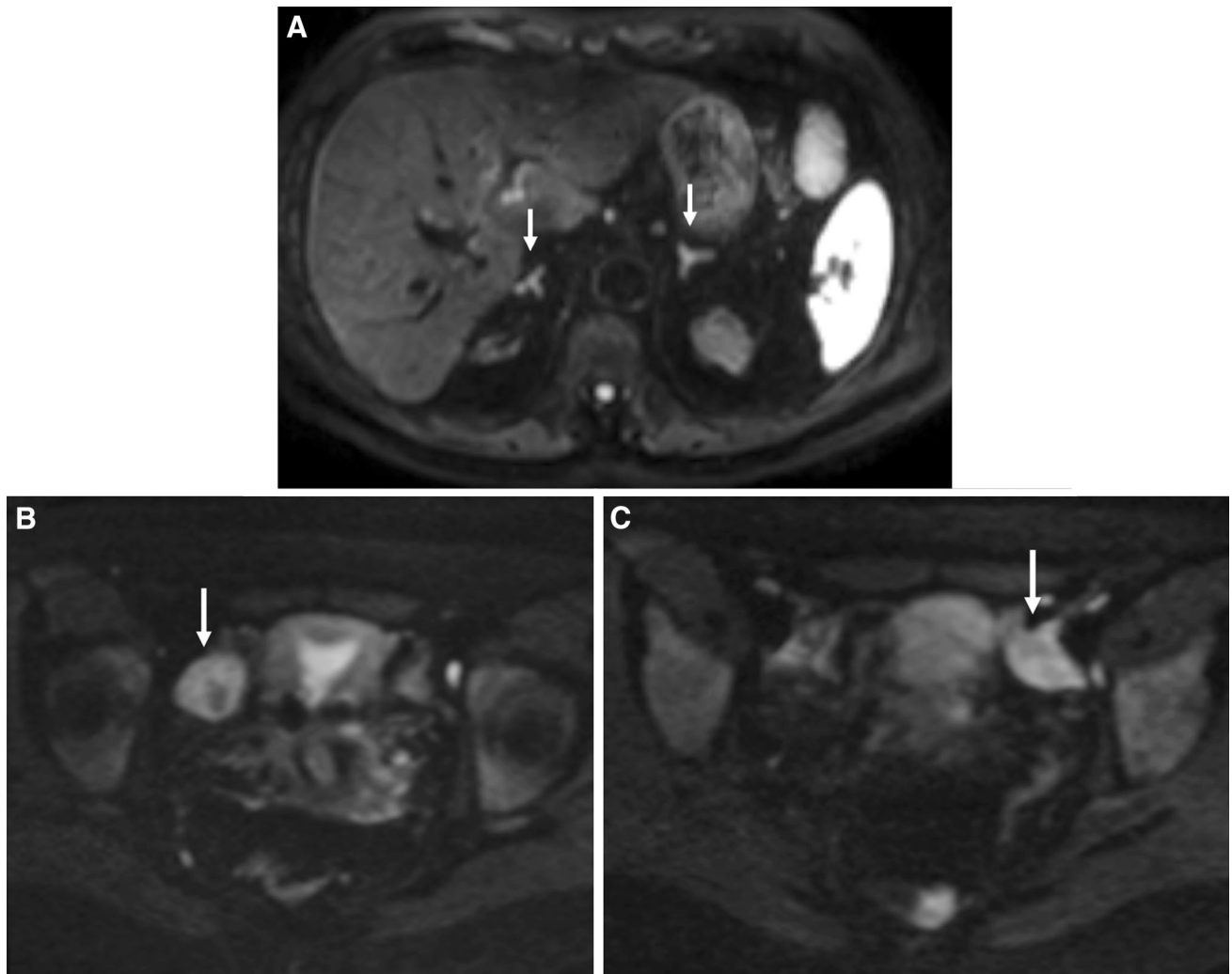


Fig. 21. Diffusion-weighted images (DWI) with a  $b$  value of 800. **A** shows normal adrenal glands bilaterally (*arrows*). **B** and **C** from a different patient show a normal right ovary in **B** and a normal left ovary in **C**. Adrenal glands (**A**) and ovaries

(**B** and **C**) are usually hyperintense on  $b = 800$  diffusion-weighted images (*arrows*) and may be more conspicuous on DWI than other pulse sequences.

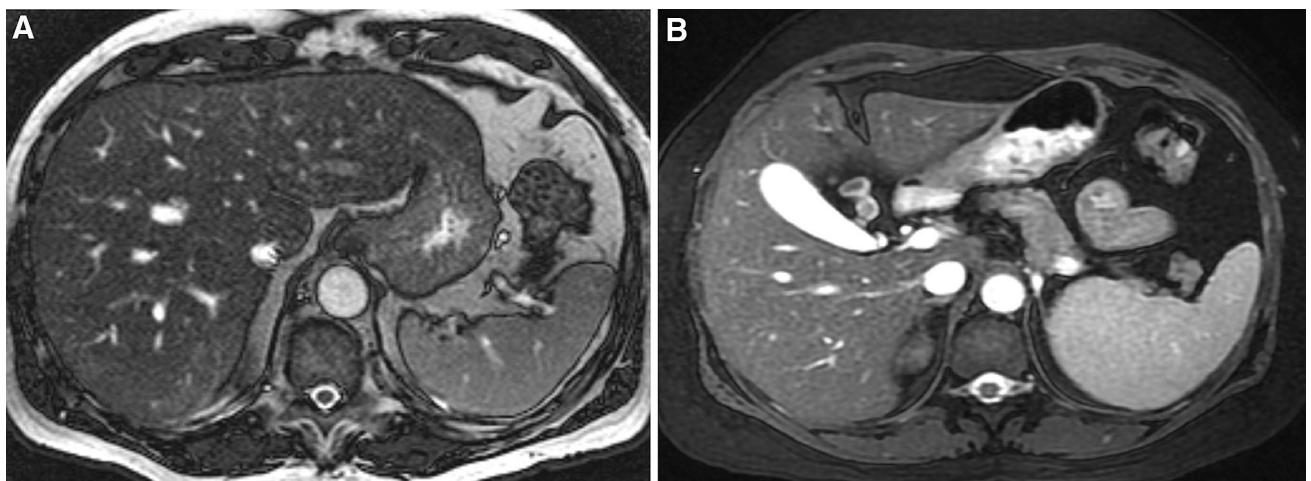
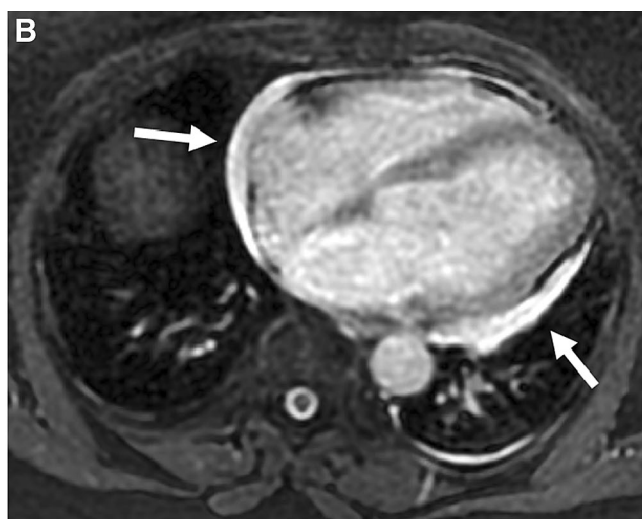
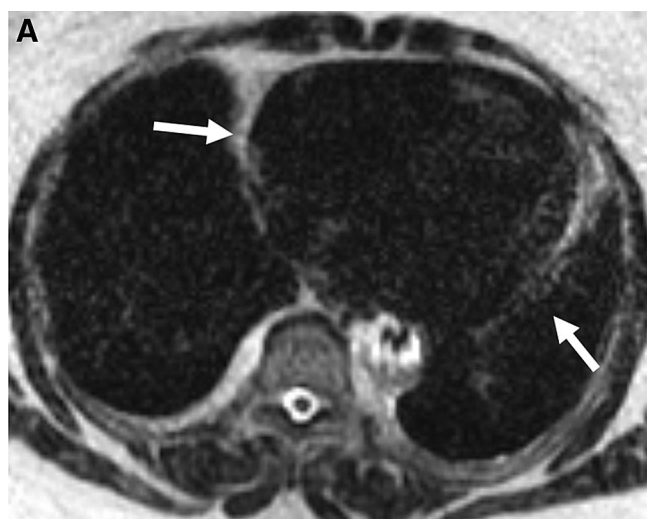
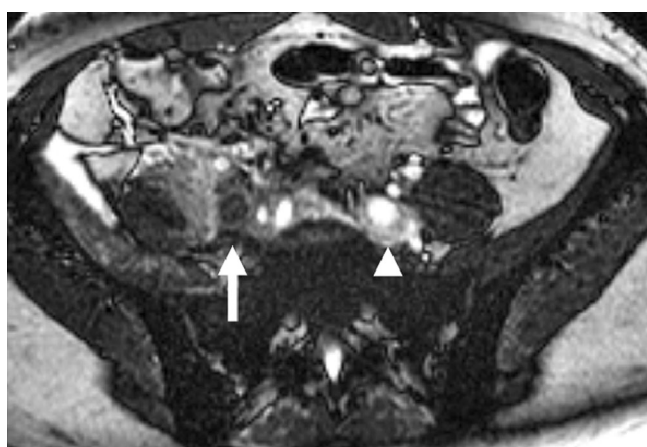


Fig. 22. Axial balanced fast-field echo image (**A**) and axial fat-suppressed fast imaging employing steady-state acquisition image (**B**).



**Fig. 23.** Heavily T2-weighted image (T2WI) with an echo time of 180 ms (**A**) and balanced steady-state free precession (BSSFP) image (**B**) in a patient with a small pericardial effu-

sion. Due to cardiac motion, the pericardial fluid is not definable on the T2WI yet readily identified on the BSSFP image.



**Fig. 24.** Balanced steady-state free precession image performed without gadolinium showing acute thrombus filling the right common iliac vein (*arrow*). The left common iliac vein is patent (*arrowhead*).

The high signal intensity of patent blood vessels on BSSFP sequences can help confirm blood vessel patency in cases where gadolinium is not used or if vessels are not optimally depicted on postcontrast images (Fig. 24) [23].

One of the limitations of BSSFP sequences is that sometimes fluid-filled structures (e.g., bile ducts and cysts) can be confused with blood vessels since they both have similar high signal intensity (Fig. 25A). Next, because a steady state of magnetization requires a highly homogeneous magnetic field, significant susceptibility artifact can be created by surgical clips or bowel gas which limits evaluation of adjacent structures (Fig. 25B) [27].

An advantage of BSSFP sequences is that in large pleural effusions or large-volume ascites, flow void arti-

facts related to fluid movement can occur with T2WI but not BSSFP [5, 26, 27].

## Dynamic multi-phase 3D gradient echo

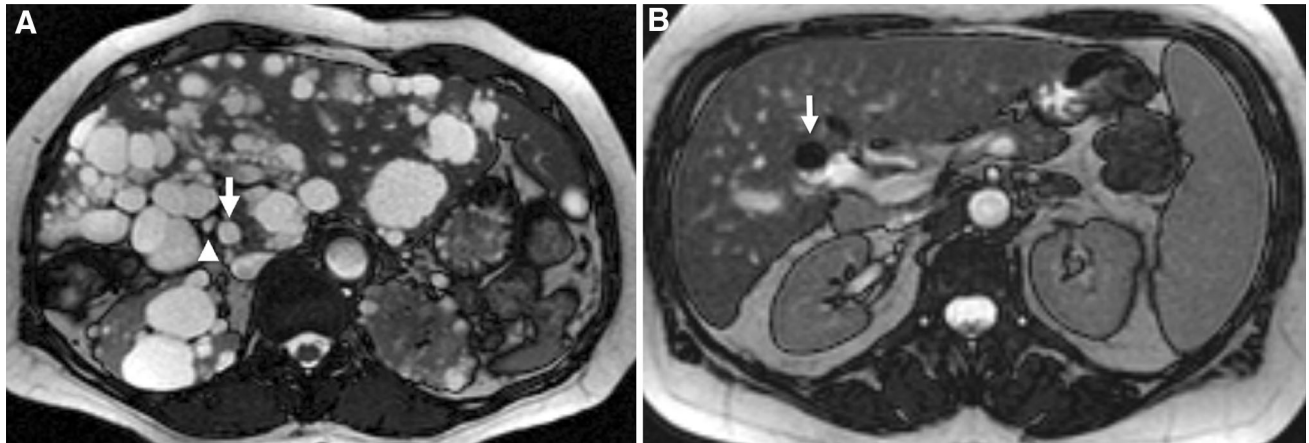
### Technique

The 3D gradient echo (3D GRE) sequence is the “work-horse” pulse sequence in an abdominal MRI protocol. Some vendor-specific terms include liver acquisition with volume acceleration (LAVA), T1 high-resolution isotropic volume excitation (THRIVE), or volumetric interpolated breath-hold examination (VIBE). Thin slices (5 mm or less) are obtained with 50% overlap. This sequence is usually fat suppressed to improve the dynamic range of the sequence. This has usually been accomplished by an intermittent fat saturation pulse, for example one per 30 or more excitations, although variable recovery of fat magnetization has been a source of some artifacts. More recently, Dixon-based techniques obviate the need for fat saturation by calculating “water images” via addition of data from in-phase and out-of-phase images [28–30]. Vendor terms for these new techniques include LAVA-Flex, modified Dixon (mDixon), and Dixon-VIBE.

### Clinical utility

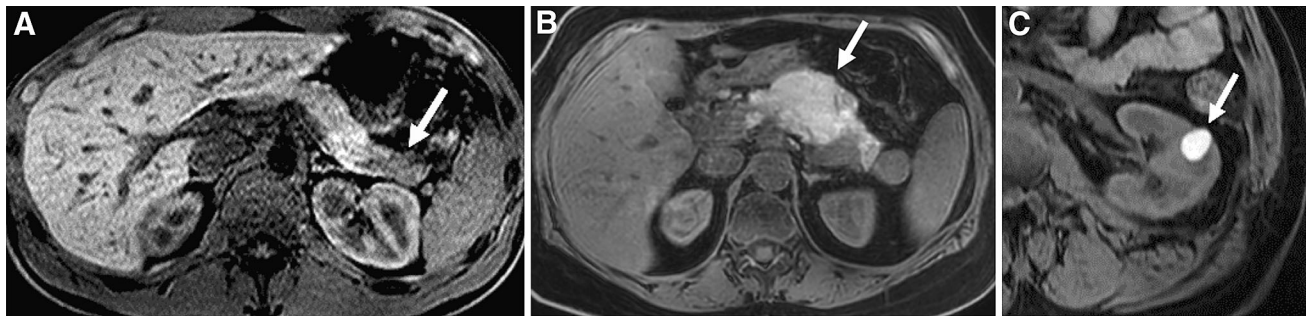
3D GRE sequences are often the most important series for tissue characterization. In addition to providing T1-weighted information, the precontrast phase of this pulse sequence identifies endogenous paramagnetic substances, such as hemorrhage or melanin (Fig. 26).

Postgadolinium, organ, lesion or blood vessel enhancement is evaluated. With 3D GRE, tissue char-



**Fig. 25.** Limitations of balanced steady-state free precession (BSSFP) sequences. **A** BSSFP image in a patient with polycystic kidney disease. Due to the multiple cysts, vascular structures such as the portal vein (*arrow*) and other fluid-filled

structures such as the extrahepatic bile duct (*arrowhead*) are not readily identifiable. **B** BSSFP image showing artifact in the gallbladder fossa from a surgical clip in a patient status post cholecystectomy (*arrow*).



**Fig. 26.** Precontrast 3D gradient echo images in 3 different patients showing (**A**) decreased T1 signal intensity from chronic pancreatitis in the distal pancreatic tail (*arrow*), **B** in-

creased signal intensity in a hemorrhagic peripancreatic collection in a patient with necrotizing pancreatitis (*arrow*), and **C** hyperintense signal in a hemorrhagic left renal cyst (*arrow*).

**Table 2.** The different categories of gadolinium-based contrast agents and the 9 commercially available contrast agents

Category	Generic name	Product or trade name	Structure	Ionicity	T1 relaxivity @ 1.5T	Hepatobiliary excretion	Concentration (mmol/mL)	Recommended dosage (mmol/kg)
Standard relaxivity macrocyclic								
ECSA	Gadoterate meglumine	Dotarem	Macrocyclic	Ionic	3.4–3.8	0	0.5	0.1
ECSA	Gadobutrol	Gadavist/ Gadovist	Macrocyclic	NonIonic	4.9–5.5	0	1	0.1
ECSA	Gadoteridol	ProHance	Macrocyclic	NonIonic	3.9–4.3	0	0.5	0.1
Standard relaxivity linear								
ECSA	Gadopentetate dimeglumine	Magnevist	Linear	Ionic	3.9–4.3	0	0.5	0.1
ECSA	Gadoversetamide	Optimark	Linear	NonIonic	4.4–5	0	0.5	0.1
ECSA	Gadodiamide	Omniscan	Linear	NonIonic	4–4.6	0	0.5	0.1
High relaxivity								
ECSA	Gadobenate dimeglumine	MultiHance	Linear	Ionic	6–6.6	3–5%	0.5	0.1
HSCA	Gadoxetate disodium	Eovist/Primovist	Linear	Ionic	6.5–7.3	50%	0.25	0.025
BPA	Gadofosveset trisodium	Ablavar/Vasovist	Linear	Ionic	18–20	9%	0.25	0.03

BPA blood pool agent, ECSA extracellular space agent, HSCA hepatocyte-specific contrast agent



**Table 3.** Suggested indications for the different categories of gadolinium-based contrast agents

Standard relaxivity ECSAs	High relaxivity ECSA (gadobenate dimeglumine)	HSCA (gadoxetate disodium)	BPA (gadofosveset trisodium)
Abdominal and/or pelvic pain Pancreas, kidney, adrenal or spleen evaluation Cirrhotic liver-HCC screening or evaluation Abdominal and/or pelvic mass Pelvic neoplasm staging Rule out appendicitis Cardiac MRI Mediastinum	MR angiography MR venography MR enterography MR urography Pelvis fistula MRI Combined abdomen and pelvis MRI	Rule out liver metastases or reevaluate known liver metastasis Characterize FNH or differentiate FNH from adenoma Cirrhotic liver-HCC screening or evaluation (alternative to ECSA) Bile duct imaging, including pre- or postsurgical evaluation <sup>a</sup> Gallbladder cystic duct obstruction <sup>a</sup>	Aortoiliac occlusive disease with known or suspected PVD Renal artery stenosis and fibromuscular dysplasia <sup>a</sup> MR venography for lower extremity DVT <sup>a</sup> Lower extremity arterial occlusive disease <sup>a</sup> AAA or dissection <sup>a</sup> Potential renal donors <sup>a</sup> AVM evaluation <sup>a</sup> Pulmonary embolism <sup>a</sup>

AAA abdominal aortic aneurysm, AVM arteriovenous malformation, BPA blood pool agent, DVT deep venous thrombosis, ECSA extracellular space agent, FNH focal nodular hyperplasia, HCC hepatocellular carcinoma, HSCA hepatocyte-specific contrast agent, PVD peripheral vascular disease

<sup>a</sup> Off-label indications

Extracellular Space Contrast Agents	Precontrast	Late Arterial Phase	Portal Venous Phase	Delayed Phase	
Gadoxetate Disodium	Precontrast	Late Arterial Phase	Portal Venous Phase	Transitional Phase	Hepatobiliary Phase

**Fig. 27.** Table showing the different contrast enhancement phases when using extracellular space contrast agents or gadoxetate disodium.



**Fig. 28.** Precontrast (A) and dynamic (B and C) and delayed (D) postcontrast 3D gradient echo images and heavily T2-weighted image with an echo time of 180 ms (E) using an

extracellular space contrast agent showing a well-defined nonenhancing liver lesion (arrows) which is T2 hyperintense (similar to CSF) consistent with a simple cyst.

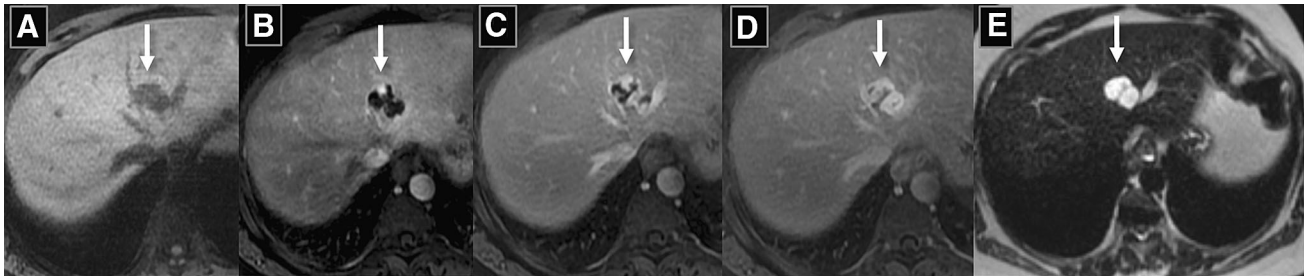
acterization is possible by obtaining multiple postcontrast enhanced phases at specified time intervals.

With 3D GRE sequences, the pattern of lesion enhancement can provide tissue characterization. Specifically:

- Early enhancement can occur with vascular structures or neoplasms.

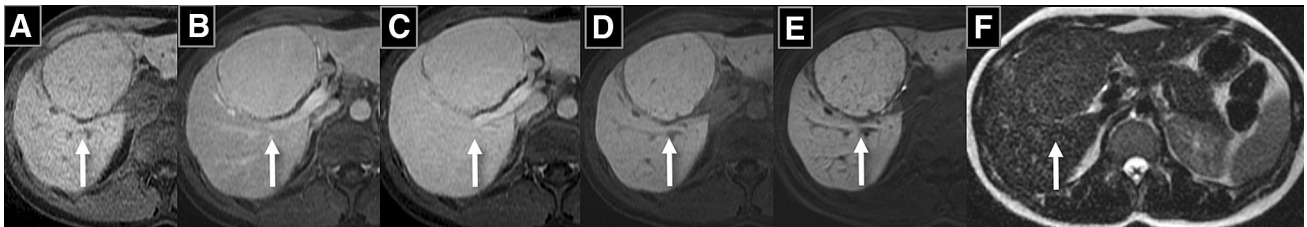
- Slow and progressive enhancement may indicate fibrosis or edema.
- Cysts or complete necrosis shows no enhancement.

To optimize interpretation of body MRI cases, having a basic understanding of the key features of the different gadolinium-based contrast agents (GBCAs) is important. Based on biodistribution, there are 3 cate-



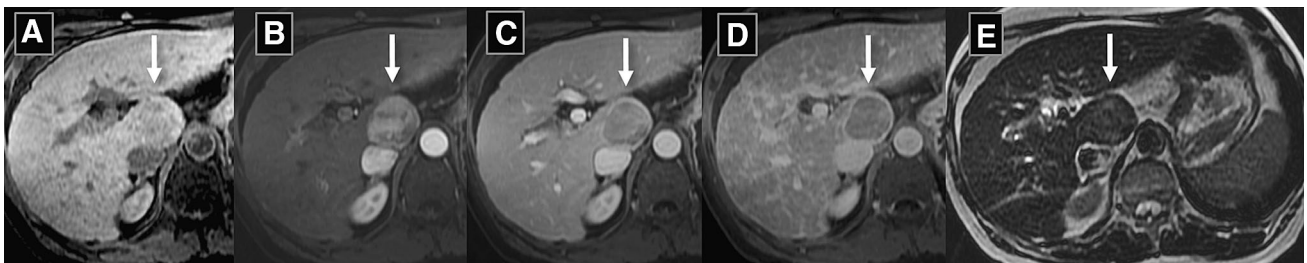
**Fig. 29.** Precontrast (A) and dynamic (B and C) and delayed (D) postcontrast 3D gradient echo images and heavily T2-weighted image (T2WI) with an echo time of 180 ms (E) using an extracellular space contrast agent showing a well-

defined liver lesion (arrows) with nodular discontinuous peripheral enhancement and progressive fill-in which is hyperintense on T2WI (similar to CSF) consistent with a hemangioma.



**Fig. 30.** Precontrast (A), dynamic postcontrast (B and C), transitional phase (D), and hepatobiliary 20 min delayed (E) 3D gradient echo images and heavily T2-weighted image with an echo time of 180 ms (F) using gadoxetate disodium showing a

well-defined homogeneously enhancing liver lesion (arrows) which is isointense to hyperintense to liver on the hepatobiliary phase and T2 isointense to mildly hyperintense with a central scar (not shown) consistent with focal nodular hyperplasia.



**Fig. 31.** Precontrast (A) and dynamic (B and C) and delayed (D) postcontrast 3D gradient echo images and heavily T2-weighted image with an echo time of 180 ms (E) using an extracellular space contrast agent in a patient with cir-

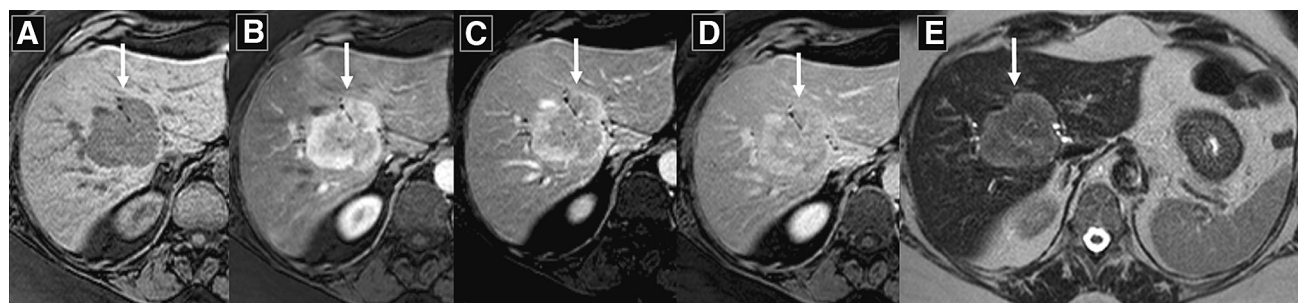
rhosis showing a heterogeneously enhancing liver lesion (arrows) with washout and a capsule appearance which is mildly T2 hyperintense consistent with hepatocellular carcinoma.

gories of GBCAs which help describe the 9 commercially available contrast agents, including extracellular space agents (ECSAs), hepatocyte-specific contrast agents (HSCAs), and blood pool agents (BPAs). ECSAs are further subcategorized into standard relaxivity macrocyclic agents, standard relaxivity linear agents, and high relaxivity linear agents. The serum protein interaction/binding of the high relaxivity linear ECSA, gadobenate dimeglumine (MultiHance; Bracco Diagnostics Inc., Princeton, NJ), leads to greater T1 shortening and increased enhancement at comparable doses compared to standard relaxivity ECSAs. Macrocyclic ECSAs are the most highly stable agents although due to the lack of serum protein binding, have similar relaxivity to the less

stable standard relaxivity linear ECSAs. Serum protein interaction/binding also accounts for increased relaxivity of the HSCA, gadoxetate disodium, and the BPA, gadofosveset trisodium (Vasovist/Ablavar; Lantheus Medical Imaging, North Billerica, MA) (Table 2) [1, 31–35].

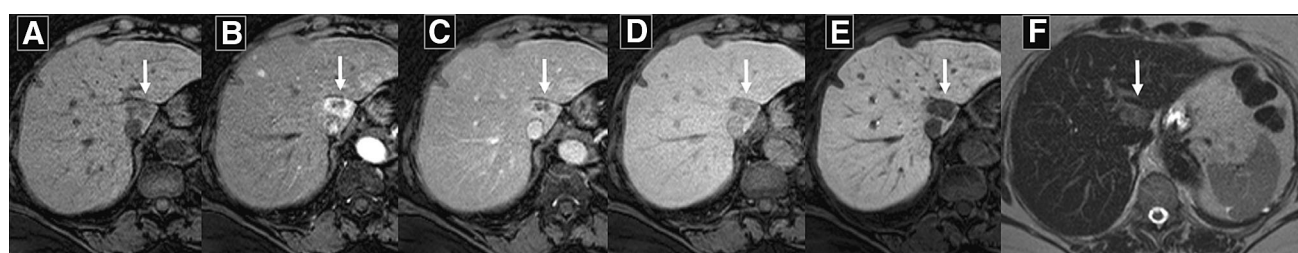
In abdominal imaging, ECSAs and HSCAs are the most commonly used GBCAs and will be the main focus of the subsequent discussion. BPAs are predominantly used for vascular applications [36, 37]. ECSAs are rapidly distributed to the extracellular space and except for gadobenate dimeglumine, have complete renal excretion [32, 38]. Gadoxetate disodium has 50% hepatobiliary excretion which makes it the default agent for hepatobiliary applications [16, 39–41]. Gadobenate dimeglu-





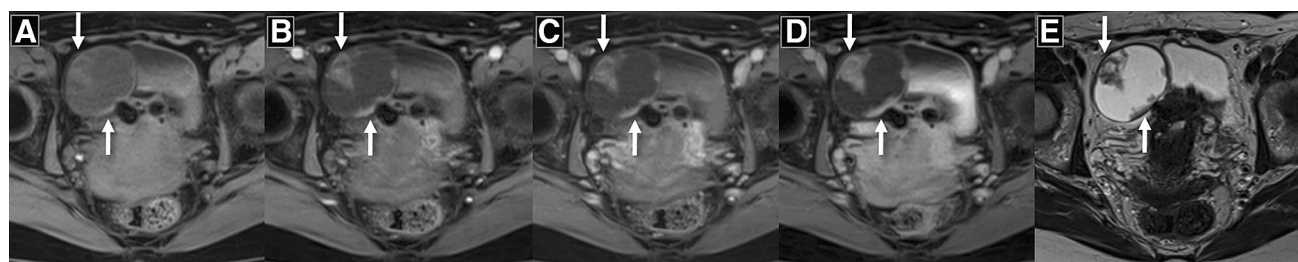
**Fig. 32.** Precontrast (A) and dynamic (B and C) and delayed (D) postcontrast 3D gradient echo images and heavily T2-weighted image with an echo time of 180 ms (E) using an extracellular space contrast agent showing a liver mass (arrows) with heterogeneous enhancement most pronounced at

the periphery and progressive centripetal enhancement and mild increased T2-signal intensity (similar to spleen). There was intrahepatic biliary duct dilatation peripheral to the lesion. Findings are consistent with mass-forming cholangiocarcinoma.



**Fig. 33.** Precontrast (A), dynamic postcontrast (B and C), transitional phase (D), and hepatobiliary 20 min delayed (E) 3D gradient echo images and heavily T2-weighted image with an echo time of 180 ms (F) using gadoxetate disodium in a patient

with metastatic uveal melanoma showing a hyperenhancing liver lesion in the caudate lobe on the late arterial phase with lack of contrast retention on the hepatobiliary phase (arrows). The lesion is mildly T2 hyperintense (similar to spleen).



**Fig. 34.** Precontrast (A) and dynamic (B and C) and delayed (D) postcontrast 3D gradient echo images and heavily T2-weighted image with an echo time of 180 ms (E) using an extracellular space contrast agent in a patient with ovarian

serous cystadenocarcinoma showing a cystic right ovarian lesion with irregular T2 hypointense mural nodules that enhance on postcontrast images (arrows).

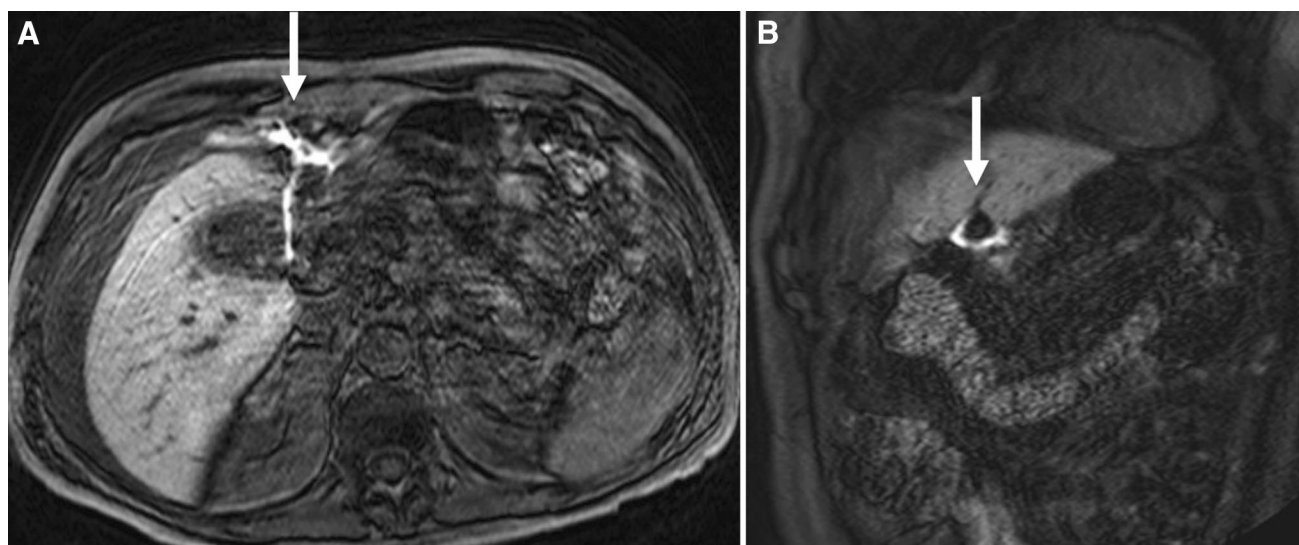
mine is also a weak hepatobiliary agent with 3–5% biliary excretion, allowing the potential for obtaining a 2-h postcontrast hepatobiliary phase [35, 39–42]. However, the most common reason to use gadobenate dimeglumine derives from its high relaxivity (due to weak protein interaction/binding) making it an appealing choice for applications where robust enhancement is critical and/or prolonged examination times require optimal enhancement, including MR angiography (MRA), MR venography (MRV), MR enterography (MRE), MR urography (MRU), pelvis fistula MRI, and combined

abdomen/pelvis MRI [2, 31, 33, 43, 44]. Suggested indications for the different gadolinium-based contrast agents are listed in Table 3.

When interpreting body MRI cases, it is important to understand the differences between ECSAs and gadoxetate disodium in both the postcontrast timing and diagnostic features of 3D gradient echo pulse sequences (Fig. 27).

- The **late arterial phase** occurs 30–35 s after injection [45–47]. During this phase, there is isolated parenchymal perfusion by the hepatic artery (prior to portal





**Fig. 35.** **A** Axial and **B** coronal 23-min delayed hepatobiliary phase 3D gradient echo images showing off-label use of gadoxetate disodium in a patient status post laparoscopic

cholecystectomy 2 weeks prior showing contrast extravasation extending anteriorly from the cystic duct region consistent with a bile leak (*arrows*).

**Table 4.** Summary of the pulse sequences discussed in this article and the clinical utility of each pulse sequence

Pulse sequence	Clinical utility
Heavily T2 weighted (TE 180–200 ms)	Cysts, fluid collections, edema, solid versus fluid, mural nodules; also fibrosis Useful to screen for benign liver lesions
Moderately T2 weighted fat suppressed (TE = 80–100 ms)	Solid masses, lymph nodes, subtle T2 contrast; also edema, inflammation
Dual gradient echo in-phase and out-of-phase	<b>Phase cancellation (out-of-phase):</b> fat mixed with water <b>Magnetic susceptibility effect (in-phase):</b> Iron, metal objects, calcium, air
2D MRCP	<b>Hyperintense on both in-phase and out-of-phase images:</b> Lipoma, hemorrhage, endometrioma
3D MRCP	Bile ducts, pancreatic ducts, gallbladder, other fluid-filled/cystic structures
Diffusion-weighted imaging	Bile ducts, pancreatic ducts, gallbladder, other fluid-filled/cystic structures <b>High b Value:</b> Solid masses, lymph nodes, bone metastases, mural nodules in cysts, abscess, normal adrenals, normal ovaries <b>Low b Value:</b> Fluid, edema, inflammation
Balanced steady-state free precession	Cysts, fluid collections, blood vessel patency, “bright-blood sequence”, cine series (MR enterography, cardiac MRI)
Dynamic multi-phase 3D gradient echo	<b>Precontrast:</b> T1-weighted information/Paramagnetic substances (e.g., low SI with chronic pancreatitis and simple cysts and high SI with hemorrhage and melanin) <b>Postcontrast:</b> Tissue characterization through enhancement patterns (e.g., <i>early enhancement</i> : vascular structures or neoplasms, <i>slow/progressive enhancement</i> : fibrosis or edema, <i>no enhancement</i> : cysts or necrosis)

2D two dimensional, 3D three dimensional, MRCP magnetic resonance cholangiopancreatography, SI signal intensity, TE echo time

venous perfusion) with enhancement of the hepatic artery and portal venous system, but not the hepatic veins. Hypervascular tissues enhance during this phase. Both ECSAs and gadoxetate disodium provide similar diagnostic information during this phase, although the latter is limited somewhat by the lower gadolinium dose administered and the more frequent occurrence of respiratory-induced motion artifact during this phase [48].

- The **portal venous phase** occurs 60–70 s after injection. Maximal hepatic enhancement occurs in this phase with ECSAs, but occurs later with gadoxetate disodium [49].

- The **delayed phase** (with ECSAs) and **transitional (or late dynamic) phase** (with gadoxetate disodium) both occur 3–5 min after injection. With ECSAs, contrast diffuses into the tissue interstitium. With gadoxetate disodium, liver enhancement continues to increase and vascular enhancement decreases more rapidly [49].
- The **hepatobiliary phase** reaches its maximum intensity approximately 20 min after injection with gadoxetate disodium, and persists for several hours. During this phase, there is maximal liver enhancement and usually biliary excretion. For off-label biliary indications, such as bile leak, obtaining images later than 20 min are generally recommended (Fig. 27) [49].

When the appropriate GBCA is used and postcontrast timing is optimized, 3D GRE sequences provide important information for tissue characterization. For example, 3D GRE sequences can help characterize several common benign lesions including cysts (Fig. 28), hemangiomas (Fig. 29), and focal nodular hyperplasia (Fig. 30) [40, 50–52].

In the proper clinical context, multiphasic 3D GRE sequences can also help characterize primary neoplasms such as hepatocellular carcinoma (Fig 31) and cholangiocarcinoma (Fig 32) [52, 53].

In the proper clinical context, 3D GRE sequences can help characterize liver metastasis (Fig. 33) [40].

On 3D GRE images, postcontrast enhancement is a feature raising concern for malignancy in cystic lesions such as ovarian and renal cystic lesions (Fig. 34) [54].

Using gadoxetate disodium, 3D GRE sequences can evaluate for a bile leak. However, it is important to obtain delayed images until the entire biliary system excretes gadolinium which may occur at or beyond the standard 20-min hepatobiliary phase. Delayed imaging beyond 20 min provides the opportunity for extravasated contrast to accumulate and increases the conspicuity of the leak and/or biloma (Fig. 35) [55].

## Conclusion

Body MRI is a powerful modality which can provide accurate and specific characterization of a variety of conditions. The interpreting radiologist initially needs to be able to recognize and reorganize pulse sequences for optimal evaluation. Next, understanding each pulse sequence's technique and clinical utility and learning how to utilize each sequence for tissue characterization is necessary (Table 4). Finally, the key features of the different categories of gadolinium-based contrast agents must be understood. After mastering these basic components, a radiologist will be capable of providing efficient and high quality interpretations of body MRI cases.

*Compliance with Ethical Standards*

*Funding* This article did not receive any funding.

*Conflict of interest* Flavius F. Guglielmo, Leann M. Kania, Christopher G. Roth, and Donald G. Mitchell declare that they have no conflict of interest. Hassan M. Ahmad is a research intern for IBM Watson Health.

*Ethical approval* This article does not contain any studies with human participants performed by any of the authors.

## References

- Ringe KI, Husarik DB, Sirlin CB, Merkle EM (2010) Gadoxetate disodium-enhanced MRI of the liver: part 1, protocol optimization and lesion appearance in the noncirrhotic liver. *Am J Roentgenol* 195:13–28
- Guglielmo FF, Mitchell DG, Gupta S (2014) Gadolinium contrast agent selection and optimal use for body mr imaging. *Radiol Clin N Am* 52:637–656
- Ito K, Mitchell DG, Outwater EK, Szklaruk J, Sadek AG (1997) Hepatic lesions: discrimination of nonsolid, benign lesions from solid, malignant lesions with heavily T2-weighted fast spin-echo MR imaging. *Radiology* 204:729–737
- Boyle GE, Ahern M, Cooke J, Sheehy NP, Meaney JF (2006) An interactive taxonomy of MR imaging sequences1. *Radiographics* 26:e24–e24
- Guglielmo FF, Mitchell DG, Roth CG, Deshmukh S (2014) Hepatic MR imaging techniques, optimization, and artifacts. *Magn Reson Imaging Clin N Am* 22:263–282
- Chang SD, Thoeni RF (2008) Effect of T1 shortening on T2-weighted MRI sequences: comparison of hepatic mass conspicuity on images acquired before and after gadolinium enhancement. *Am J Roentgenol* 190:1318–1323
- Jeong YY, Mitchell DG, Holland GA (2001) Liver lesion conspicuity: T2-weighted Breath-hold fast spin-echo MR imaging before and after gadolinium enhancement—initial experience1. *Radiology* 219:455–460
- Pokhare SS, Macura KJ, Kamel IR, Zaheer A (2013) Current MR imaging lipid detection techniques for diagnosis of lesions in the abdomen and pelvis. *Radiographics* 33(3):681–702
- Earls JP, Krinsky GA (1997) Abdominal and pelvic applications of opposed-phase MR imaging. *AJR Am J Roentgenol* 169:1071–1077
- Delfaut EM, Beltran J, Johnson G, et al. (1999) Fat suppression in MR imaging: techniques and pitfalls. *Radiographics* 19:373–382
- Cassidy FH, Yokoo T, Aganovic L, et al. (2009) fatty liver disease: MR imaging techniques for the detection and quantification of liver steatosis 1. *Radiographics* 29:231–260
- Merkle EM, Nelson RC (2006) Dual gradient-echo in-phase and opposed-phase hepatic mr imaging: a useful tool for evaluating more than fatty infiltration or fatty sparing 1. *Radiographics* 26:1409–1418
- Bitar R, Leung G, Perng R, et al. (2006) MR pulse sequences: what every radiologist wants to know but is afraid to ask 1. *Radiographics* 26:513–537
- Griffin N, Charles-Edwards G, Grant LA (2012) Magnetic resonance cholangiopancreatography: the ABC of MRCP. *Insights Imaging* 3:11–21
- Takahashi S, Kim T, Murakami T, et al. (2000) Influence of paramagnetic contrast on single-shot MRCP image quality. *Abdom Imaging* 25:511–513
- Van Beers BE, Pastor CM, Hussain HK (2012) Primovist, Eovist: what to expect? *J Hepatol* 57(2):421–429
- Dietrich O, Biffar A, Baur-Melnyk A, Reiser MF (2010) Technical aspects of MR diffusion imaging of the body. *Eur J Radiol* 76:314–322
- Koh D, Collins DJ (2007) Diffusion-weighted MRI in the body: applications and challenges in oncology. *Am J Roentgenol* 188:1622–1635
- Malayeri AA, El Khouli RH, Zaheer A, et al. (2011) Principles and applications of diffusion-weighted imaging in cancer detection, staging, and treatment follow-up. *Radiographics* 31:1773–1791
- Taouli B, Koh D (2010) Diffusion-weighted MR imaging of the liver1. *Radiology* 254:47–66
- Koh D, Takahara T, Imai Y, Collins DJ (2007) Practical aspects of assessing tumors using clinical diffusion-weighted imaging in the body. *Magn Reson Med Sci* 6:211–224
- Parikh T, Drew SJ, Lee VS, et al. (2008) Focal liver lesion detection and characterization with diffusion-weighted mr imaging: comparison with standard breath-hold T2-weighted imaging 1. *Radiology* 246:812–822
- Chavhan GB, Babyn PS, Jankharia BG, Cheng HM, Shroff MM (2008) Steady-state MR imaging sequences: physics, classification, and clinical applications1. *Radiographics* 28:1147–1160
- Hargreaves B (2004) Fast gradient echo sequences including balanced SSFP. *J Magn Reson Imaging* 20:857–864
- Scheffler K, Lehnhardt S (2003) Principles and applications of balanced SSFP techniques. *Eur Radiol* 13:2409–2418
- Graves MJ, Mitchell DG (2013) Body MRI artifacts in clinical practice: a physicist's and radiologist's perspective. *J Magn Reson Imaging* 38:269–287
- Rescinito G, Sirlin C, Cittadini G Jr (2009) Body MRI artefacts: from image degradation to diagnostic utility. *Radiol Med* 114:18–31

28. Ma J (2004) Breath-hold water and fat imaging using a dual-echo two-point dixon technique with an efficient and robust phase-correction algorithm. *Magn Reson Med* 52:415–419
29. Ma J, Vu AT, Son JB, Choi H, Hazle JD (2006) Fat-suppressed three-dimensional dual echo dixon technique for contrast agent enhanced MRI. *J Magn Reson Imaging* 23:36–41
30. Ma J (2008) Dixon techniques for water and fat imaging. *J Magn Reson Imaging* 28:543–558
31. Hao D, Ai T, Goerner F, et al. (2012) MRI contrast agents: basic chemistry and safety. *J Magn Reson Imaging* 36:1060–1071
32. van der Molen AJ, Bellin MF (2008) Extracellular gadolinium-based contrast media: differences in diagnostic efficacy. *Eur J Radiol* 66:168–174
33. Tweedle MF, Kanal E, Muller R (2014) Considerations in the selection of a new gadolinium-based contrast agent. *Appl Radiol (Suppl)*:1–11
34. Prince MR, Zhang HL, Roditi GH, Leiner T, Kucharczyk W (2009) Risk factors for NSF: a literature review. *J Magn Reson Imaging* 30:1298–1308
35. Frydrychowicz A, Lubner MG, Brown JJ, et al. (2012) Hepatobiliary MR imaging with gadolinium-based contrast agents. *J Magn Reson Imaging* 35:492–511
36. Hadizadeh DR, Gieseke J, Lohmaier SH, et al. (2008) Peripheral MR angiography with blood pool contrast agent: prospective intraindividual comparative study of high-spatial-resolution steady-state MR angiography versus standard-resolution first-pass MR angiography and DSA1. *Radiology* 249:701–711
37. Lewis M, Yanny S, Malcolm PN (2012) Advantages of blood pool contrast agents in MR angiography: a pictorial review. *J Med Imaging Radiat Oncol* 56:187–191
38. Morcos S (2008) Extracellular gadolinium contrast agents: differences in stability. *Eur J Radiol* 66:175–179
39. Gandhi SN, Brown MA, Wong JG, Aguirre DA, Sirlin CB (2006) MR contrast agents for liver imaging: what, when, how1. *Radiographics* 26:1621–1636
40. Seale MK, Catalano OA, Saini S, Hahn PF, Sahani DV (2009) Hepatobiliary-specific MR contrast agents: role in imaging the liver and biliary tree. *Radiographics* 29:1725–1748
41. Goodwin MD, Dobson JE, Sirlin CB, Lim BG, Stella DL (2011) Diagnostic challenges and pitfalls in MR imaging with hepatocyte-specific contrast agents. *Radiographics* 31:1547–1568
42. Shellock FG, Parker JR, Pirovano G, et al. (2006) Safety characteristics of gadobenate dimeglumine: clinical experience from intra- and interindividual comparison studies with gadopentetate dimeglumine. *J Magn Reson Imaging* 24:1378–1385
43. Gerretsen SC, le Maire TF, Miller S, et al. (2010) Multicenter, double-blind, randomized, intraindividual crossover comparison of gadobenate dimeglumine and gadopentetate dimeglumine for MR angiography of peripheral arteries 1. *Radiology* 255:988–1000
44. Pintaske J, Martirosian P, Graf H, et al. (2006) Relaxivity of gadopentetate dimeglumine (Magnevist), gadobutrol (Gadovist), and gadobenate dimeglumine (MultiHance) in human blood plasma at 0.2, 1.5, and 3 Tesla. *Investig Radiol* 41:213–221
45. Hussain HK, Londy FJ, Francis IR, et al. (2003) Hepatic arterial phase mr imaging with automated bolus-detection three-dimensional fast gradient-recalled-echo sequence: comparison with test-bolus method 1. *Radiology* 226:558–566
46. Mitchell D, Cohen M (2004) *MRI principles*. Philadelphia: Elsevier
47. Semelka RC, Helmberger TKG (2001) Contrast agents for MR imaging of the liver1. *Radiology* 218:27–38
48. Davenport MS, Vigiante BL, Al-Hawary MM, et al. (2013) Comparison of acute transient dyspnea after intravenous administration of gadoxetate disodium and gadobenate dimeglumine: effect on arterial phase image quality. *Radiology* 266:452–461
49. American College of Radiology. Liver Imaging Reporting and Data System version 2014. <http://www.acr.org/Quality-Safety/Resources/LIRADS/>. Accessed 6 Mar 2016
50. Klotz T, Montoriol P, Da Ines D, et al. (2013) Hepatic haemangioma: common and uncommon imaging features. *Diagn Interv Imaging* 94:849–859
51. Cogley JR, Miller FH (2014) MR imaging of benign focal liver lesions. *Radiol Clin N Am* 52:657–682
52. Siegelman ES, Chauhan A (2014) MR characterization of focal liver lesions: pearls and pitfalls. *Magn Reson Imaging Clin N Am* 22:295–313
53. Péporté AR, Sommer WH, Nikolaou K, Reiser MF, Zech CJ (2013) Imaging features of intrahepatic cholangiocarcinoma in Gd-EOB-DTPA-enhanced MRI. *Eur J Radiol* 82:e101–e106
54. Zhang P, Cui Y, Li W, et al. (2012) Diagnostic accuracy of diffusion-weighted imaging with conventional MR imaging for differentiating complex solid and cystic ovarian tumors at 1.5 T. *World J Surg Oncol* 10:237
55. Ratcliffe GE, Kirkpatrick ID (2014) Anik Sahni V, Greenberg HM, Henderson B, Radulovic D, Mottola JC. Detection and localization of bile duct leaks after cholecystectomy using Gd-EOB-DTPA-enhanced MR cholangiography: retrospective study of 16 patients. *J Comput Assist Tomogr* 38:518–525